

High Order Weighted Essentially Non-Oscillatory Schemes for Convection Dominated Problems

Chi-Wang Shu¹

Division of Applied Mathematics, Brown University, Providence, Rhode Island 02912

ABSTRACT

High order accurate weighted essentially non-oscillatory (WENO) schemes are relatively new but have gained rapid popularity in numerical solutions of hyperbolic partial differential equations and other convection dominated problems. The main advantage of such schemes is their capability to achieve arbitrarily high order formal accuracy in smooth regions while maintaining stable, non-oscillatory and sharp discontinuity transitions. The schemes are thus especially suitable for problems containing both strong discontinuities and complex smooth solution features. WENO schemes are robust and do not require the users to tune parameters, thus they are very convenient to use for practitioners. In this paper we review the history and basic formulation of WENO schemes, outline the main ideas in using WENO schemes to solve various hyperbolic partial differential equations and other convection dominated problems, and present a collected sample of applications in areas including computational fluid dynamics, computational astronomy and astrophysics, semiconductor device simulation, traffic flow models, and computational biology. Finally, we mention a few topics currently being investigated about WENO schemes.

Key Words: Weighted essentially non-oscillatory (WENO) scheme, hyperbolic partial differential equations, convection dominated problems, computational fluid dynamics, computational astronomy and astrophysics, semiconductor device simulation, traffic flow models, computational biology

AMS(MOS) subject classification: 65M06

¹E-mail: shu@dam.brown.edu. Research supported by ARO grant W911NF-04-1-0291, NSF grants DMS-0510345 and AST-0506734, and AFOSR grant FA9550-05-1-0123.

1 Introduction

In this paper we review a relatively recent yet quite popular class of high order numerical methods for solving convection dominated partial differential equations (PDEs), in particular hyperbolic conservation laws. This class of schemes is termed weighted essentially non-oscillatory, or WENO schemes. The first WENO scheme was introduced in 1994 by Liu, Osher and Chan in their pioneering paper [101], in which a third order accurate finite volume WENO scheme was designed. In 1996, Jiang and Shu [76] provided a general framework to construct arbitrary order accurate finite difference WENO schemes, which are more efficient for multi-dimensional calculations. Most of the applications use the fifth order accurate WENO scheme designed in [76], which has been cited 331 times as of December 30, 2006 according to the ISI Web of Science database. The papers which cited [76] are from 83 different journals, most of them being application journals.

For convection dominated problems, especially for hyperbolic conservation laws, the main challenge to the design of numerical schemes is the presence of discontinuities (such as shocks and contact discontinuities in high speed gas dynamics) or sharp transition layers. This happens often in complex solution structures including also smooth components such as vortices and acoustic waves. Traditional low order numerical methods, such as the first order Godunov scheme [50] or Roe scheme [132], can resolve the discontinuities monotonically without spurious numerical oscillations, however they often smear some of these discontinuities (for example the contact discontinuities) excessively. They also contain relatively large numerical dissipation in the smooth part of the solution, hence many grid points are required to resolve complicated smooth structures such as vortices and acoustic waves, especially for long time simulation. The so-called high resolution schemes designed in the 1970s and 1980s, represented by the MUSCL schemes [157], TVD schemes [61], and PPM schemes [33], are usually second order accurate in smooth regions, and can resolve discontinuities monotonically with a sharper transition than first order schemes. These high resolution schemes are very popular in applications. They are often the best choice in terms of a balance between computer cost

and desired resolution, especially for problems with solutions dominated by shocks or other discontinuities with relatively simple structures between these discontinuities. For problems containing both shocks and complicated *smooth* solution structure, such as shock interaction with vortices or acoustic waves, schemes with higher order of accuracy which can resolve shocks in an essentially non-oscillatory fashion is desirable. A successful class of such high order schemes is the class of essentially non-oscillatory, or ENO schemes [64, 146, 147]. ENO schemes can be designed for any order of accuracy, and they produce sharp and essentially non-oscillatory shock transitions even for strong shocks. WENO schemes are constructed based on the successful ENO schemes with additional advantages, which explains their rapid gaining of widespread popularity in applications. Many of the details regarding WENO schemes can be found in the lecture notes [142, 143].

The essential idea of the WENO schemes is an adaptive interpolation or reconstruction procedure. This is explained in detail in Section 2. In Section 3 we describe the finite difference and finite volume WENO schemes for solving hyperbolic conservation laws. We start with the simple one dimensional scalar case and then remark on the necessary procedures to generalize the algorithm to handle systems, multi-space dimensions including unstructured meshes, boundary conditions and time discretization. In Section 4 we describe finite difference WENO schemes for solving the Hamilton-Jacobi equations on structured and unstructured meshes. In Section 5 we describe the relationship between the WENO schemes and a few other classes of high order schemes for convection dominated problems, including the discontinuous Galerkin methods, compact schemes, spectral methods, wavelets and multi-resolution methods, and dispersion optimized finite difference schemes for wave propagation problems. Rather than surveying the details of these methods, we emphasize efforts in combining the advantages of these methods and the WENO procedure. Section 6 contains a collected sample of the application of WENO schemes in science and engineering, in diverse areas including computational fluid dynamics, computational astronomy and astrophysics, semiconductor device simulation, traffic flow models, and computational biology. Finally, in

Section 7 we mention a few topics currently being investigated about WENO schemes.

2 WENO interpolation and reconstruction

At the heart of the WENO schemes is actually an approximation problem, not directly related to PDEs. In this section we will use simple examples to describe this approximation problem.

2.1 WENO interpolation

We first look at the problem of interpolation. Assume that we have a mesh $\dots < x_1 < x_2 < x_3 < \dots$. Further assume, for simplicity, that the mesh is uniform, i.e. $\Delta x = x_{i+1} - x_i$ is a constant. Therefore we may take $x_i = i \Delta x$. We assume that we are given the point values of a function $u(x)$ at the grid points in this mesh, that is, $u_i = u(x_i)$ is known for all i . We would like to find an approximation of the function $u(x)$ at a point other than the nodes x_i , for example at the half nodes $x_{i+\frac{1}{2}}$.

This can be handled by the traditional approach of interpolation. For example, we could find a unique polynomial of degree at most two, denoted by $p_1(x)$, which interpolates the function $u(x)$ at the mesh points in the stencil $S_1 = \{x_{i-2}, x_{i-1}, x_i\}$. That is, we have $p_1(x_j) = u_j$ for $j = i-2, i-1, i$. We could then use $u_{i+\frac{1}{2}}^{(1)} \equiv p_1(x_{i+\frac{1}{2}})$ as an approximation to the value $u(x_{i+\frac{1}{2}})$. A simple algebra leads to the explicit formula for this approximation

$$u_{i+\frac{1}{2}}^{(1)} = \frac{3}{8}u_{i-2} - \frac{5}{4}u_{i-1} + \frac{15}{8}u_i \quad (2.1)$$

From elementary numerical analysis, we know that this approximation is third order accurate

$$u_{i+\frac{1}{2}}^{(1)} - u(x_{i+\frac{1}{2}}) = O(\Delta x^3)$$

if the function $u(x)$ is smooth in the stencil S_1 . Similarly, if we choose a different stencil $S_2 = \{x_{i-1}, x_i, x_{i+1}\}$, we would obtain a different interpolation polynomial $p_2(x)$ satisfying $p_2(x_j) = u_j$ for $j = i-1, i, i+1$. We then obtain a different approximation $u_{i+\frac{1}{2}}^{(2)} \equiv p_2(x_{i+\frac{1}{2}})$

to $u(x_{i+\frac{1}{2}})$, given explicitly as

$$u_{i+\frac{1}{2}}^{(2)} = -\frac{1}{8}u_{i-1} + \frac{3}{4}u_i + \frac{3}{8}u_{i+1}, \quad (2.2)$$

which is also third order accurate

$$u_{i+\frac{1}{2}}^{(2)} - u(x_{i+\frac{1}{2}}) = O(\Delta x^3)$$

provided that the function $u(x)$ is smooth in the stencil S_2 . Finally, a third stencil $S_3 = \{x_i, x_{i+1}, x_{i+2}\}$ would lead to yet another different interpolation polynomial $p_3(x)$, satisfying $p_3(x_j) = u_j$ for $j = i, i+1, i+2$ and giving another approximation $u_{i+\frac{1}{2}}^{(3)} \equiv p_3(x_{i+\frac{1}{2}})$, or explicitly as

$$u_{i+\frac{1}{2}}^{(3)} = \frac{3}{8}u_i + \frac{3}{4}u_{i+1} - \frac{1}{8}u_{i+2}, \quad (2.3)$$

which is of course also third order accurate

$$u_{i+\frac{1}{2}}^{(3)} - u(x_{i+\frac{1}{2}}) = O(\Delta x^3)$$

provided that the function $u(x)$ is smooth in the stencil S_3 .

If the function $u(x)$ is globally smooth, all three approximations $u_{i+\frac{1}{2}}^{(1)}$, $u_{i+\frac{1}{2}}^{(2)}$ and $u_{i+\frac{1}{2}}^{(3)}$ obtained above are third order accurate. One could choose one of them based on other considerations, for example to make the coefficient of the error term $O(\Delta x^3)$ as small as possible (which would then favor the more symmetric approximations $u_{i+\frac{1}{2}}^{(2)}$ or $u_{i+\frac{1}{2}}^{(3)}$ over $u_{i+\frac{1}{2}}^{(1)}$). For using them to design finite difference approximations for solving time dependent PDEs, the choice of these stencils would also need to be restricted by the linear stability of the resulting scheme.

If we use the large stencil $S = \{x_{i-2}, x_{i-1}, x_i, x_{i+1}, x_{i+2}\}$, which is the union of all three third order stencils S_1 , S_2 and S_3 , then we would be able to obtain an interpolation polynomial $p(x)$ of degree at most four, satisfying $p(x_j) = u_j$ for $j = i-2, i-1, i, i+1, i+2$, and giving an approximation $u_{i+\frac{1}{2}} \equiv p(x_{i+\frac{1}{2}})$, or explicitly as

$$u_{i+\frac{1}{2}} = \frac{3}{128}u_{i-2} - \frac{5}{32}u_{i-1} + \frac{45}{64}u_i + \frac{15}{32}u_{i+1} - \frac{5}{128}u_{i+2}, \quad (2.4)$$

which is fifth order accurate

$$u_{i+\frac{1}{2}} - u(x_{i+\frac{1}{2}}) = O(\Delta x^5)$$

provided that the function $u(x)$ is smooth in the large stencil S .

An important observation, which will be used later in our WENO interpolation, is that the fifth order approximation $u_{i+\frac{1}{2}}$, defined in (2.4) and based on the large stencil S , can be written as a linear convex combination of the three third order approximations $u_{i+\frac{1}{2}}^{(1)}$, $u_{i+\frac{1}{2}}^{(2)}$ and $u_{i+\frac{1}{2}}^{(3)}$, defined by (2.1), (2.2), (2.3) and based on the three small stencils S_1 , S_2 and S_3 respectively:

$$u_{i+\frac{1}{2}} = \gamma_1 u_{i+\frac{1}{2}}^{(1)} + \gamma_2 u_{i+\frac{1}{2}}^{(2)} + \gamma_3 u_{i+\frac{1}{2}}^{(3)} \quad (2.5)$$

where the constants γ_1 , γ_2 and γ_3 , satisfying $\gamma_1 + \gamma_2 + \gamma_3 = 1$ and usually referred to as the *linear weights* in the WENO literature, are given in this case as

$$\gamma_1 = \frac{1}{16}, \quad \gamma_2 = \frac{5}{8}, \quad \gamma_3 = \frac{5}{16}.$$

Now we assume that $u(x)$ is only piecewise smooth and is discontinuous at isolated points. For such a function $u(x)$, if Δx is small enough so that the large stencil S does not contain two discontinuity points of $u(x)$, then for each index i we have the following three possibilities

1. The function $u(x)$ is smooth in the big stencil S . In this case, all three third order approximations $u_{i+\frac{1}{2}}^{(1)}$, $u_{i+\frac{1}{2}}^{(2)}$ and $u_{i+\frac{1}{2}}^{(3)}$ can be used, as well as the fifth order approximation $u_{i+\frac{1}{2}}$ given by (2.4) or by (2.5).
2. The function $u(x)$ has a discontinuity point in $[x_{i-2}, x_i]$ or in $(x_{i+1}, x_{i+2}]$. In this case there is at least one stencil out of S_1 , S_2 and S_3 in which the function $u(x)$ is smooth. That is, at least one of the three third order approximations $u_{i+\frac{1}{2}}^{(1)}$, $u_{i+\frac{1}{2}}^{(2)}$ and $u_{i+\frac{1}{2}}^{(3)}$ is still a valid third order accurate approximation to $u(x_{i+\frac{1}{2}})$.
3. The function $u(x)$ has a discontinuity point in $[x_i, x_{i+1}]$. In this case all three small stencils S_1 , S_2 and S_3 will contain the discontinuity.

For this interpolation problem, the third case above can be avoided if we add another third order stencil $S_4 = \{x_{i+1}, x_{i+2}, x_{i+3}\}$ into consideration. Unfortunately, for solving PDEs and because of the requirement of conservation, it is usually not possible to avoid this case. However, the good news is that this seemingly difficult case is actually not problematic. This is because the interpolation polynomial $p(x)$, as well as $p_1(x)$, $p_2(x)$ and $p_3(x)$, are all essentially monotone in the interval $[x_i, x_{i+1}]$. That is, no spurious overshoot or undershoot would appear in this interval $[x_i, x_{i+1}]$ which contains a discontinuity of $u(x)$. To demonstrate this fact, let us assume for simplicity that $u_j = 1$ for $j \leq i$ and $u_j = 0$ for $j \geq i + 1$, that is, $u(x)$ is a step function with a discontinuity in $[x_i, x_{i+1}]$. The polynomial $p(x)$ interpolates $u(x)$ in the stencil S , that is, $p(x_{i-2}) = p(x_{i-1}) = p(x_i) = 1$, and $p(x_{i+1}) = p(x_{i+2}) = 0$. Therefore, there is at least one zero of $p'(x)$ in each of the intervals (x_{i-2}, x_{i-1}) , (x_{i-1}, x_i) and (x_{i+1}, x_{i+2}) . However, $p'(x)$ is a polynomial of degree at most three, so it has at most three distinct zeros, which are all accounted for in the three intervals above. We thus conclude that $p'(x)$ does *not* have a zero in the interval $[x_i, x_{i+1}]$, hence $p(x)$ is monotone in this interval. This result also holds when $u(x)$ is a more general piecewise smooth function [65]. Therefore, the interpolation to $u(x_{i+\frac{1}{2}})$ in this case will *not* be oscillatory, even though it may not be accurate.

The classical ENO idea to treat the first two cases above is to choose *one of* the three approximations $u_{i+\frac{1}{2}}^{(1)}$, $u_{i+\frac{1}{2}}^{(2)}$ and $u_{i+\frac{1}{2}}^{(3)}$, defined by (2.1), (2.2), (2.3) and based on the three stencils S_1 , S_2 and S_3 respectively, using the information of the local smoothness of the given data u_j for $i - 2 \leq j \leq i + 2$. This would guarantee third order accuracy and essentially non-oscillatory performance since $u(x)$ is smooth in at least one of the three stencils S_1 , S_2 and S_3 .

On the other hand, the WENO idea is to choose the final approximation as a convex combination of the three third order approximations $u_{i+\frac{1}{2}}^{(1)}$, $u_{i+\frac{1}{2}}^{(2)}$ and $u_{i+\frac{1}{2}}^{(3)}$:

$$u_{i+\frac{1}{2}} = w_1 u_{i+\frac{1}{2}}^{(1)} + w_2 u_{i+\frac{1}{2}}^{(2)} + w_3 u_{i+\frac{1}{2}}^{(3)} \quad (2.6)$$

where $w_j \geq 0$, $w_1 + w_2 + w_3 = 1$. Notice that for the third case above, the WENO ap-

proximation $u_{i+\frac{1}{2}}$ is still monotone, since it is a convex combination of three monotone approximations. We would hope that the *nonlinear weights* w_j satisfy the following requirements

- $w_j \approx \gamma_j$ if $u(x)$ is smooth in the big stencil S .
- $w_j \approx 0$ if $u(x)$ has a discontinuity in the stencil S_j but it is smooth in at least one of the other two stencils.

It can be verified [76] that, as long as $w_j = \gamma_j + O(\Delta x^2)$, the WENO interpolation $u_{i+\frac{1}{2}}$ is fifth order accurate

$$u_{i+\frac{1}{2}} - u(x_{i+\frac{1}{2}}) = O(\Delta x^5)$$

when the function $u(x)$ is smooth in the large stencil S , namely in the first case above, just as the original linear interpolation given by (2.4) or by (2.5). The second requirement above would guarantee a non-oscillatory, at least third order accurate WENO approximation $u_{i+\frac{1}{2}}$ given by (2.6) in the second case above, since the contribution from any stencil containing the discontinuity of $u(x)$ has an essentially zero weight. In our choice of the WENO weights below, $w_j = O(\Delta x^4)$.

The choice of the nonlinear weights w_j relies on the *smoothness indicator* β_j , which measures the relative smoothness of the function $u(x)$ in the stencil S_j . The larger this smoothness indicator β_j , the less smooth the function $u(x)$ is in the stencil S_j . In most of the WENO papers, this smoothness indicator is chosen as in [76]

$$\beta_j = \sum_{l=1}^k \Delta x^{2l-1} \int_{x_{i-\frac{1}{2}}}^{x_{i+\frac{1}{2}}} \left(\frac{d^l}{dx^l} p_j(x) \right)^2 dx \quad (2.7)$$

where k is the polynomial degree of $p_j(x)$ (in our example $k = 2$). This is clearly just a scaled sum of the square L^2 norms of all the derivatives of the relevant interpolation polynomial $p_j(x)$ in the relevant interval $[x_{i-\frac{1}{2}}, x_{i+\frac{1}{2}}]$ where the interpolating point is located. The scaling factor Δx^{2l-1} is to make sure that the final explicit formulas for the smoothness indicators

do not depend on the mesh size Δx . In our example, we can easily work out these explicit formulas as

$$\begin{aligned}\beta_1 &= \frac{1}{3} (4u_{i-2}^2 - 19u_{i-2}u_{i-1} + 25u_{i-1}^2 + 11u_{i-2}u_i - 31u_{i-1}u_i + 10u_i^2) \\ \beta_2 &= \frac{1}{3} (4u_{i-1}^2 - 13u_{i-1}u_i + 13u_i^2 + 5u_{i-1}u_{i+1} - 13u_iu_{i+1} + 4u_{i+1}^2) \\ \beta_3 &= \frac{1}{3} (10u_i^2 - 31u_iu_{i+1} + 25u_{i+1}^2 + 11u_iu_{i+2} - 19u_{i+1}u_{i+2} + 4u_{i+2}^2)\end{aligned}\quad (2.8)$$

Notice that these smoothness indicators are quadratic functions of the values of $u(x)$ in the relevant stencils. Equipped with these smoothness indicators, we can now define the nonlinear weights as

$$w_j = \frac{\tilde{w}_j}{\tilde{w}_1 + \tilde{w}_2 + \tilde{w}_3}, \quad \text{with} \quad \tilde{w}_j = \frac{\gamma_j}{(\varepsilon + \beta_j)^2}. \quad (2.9)$$

Here ε is a small positive number to avoid the denominator to become zero is typically chosen as $\varepsilon = 10^{-6}$ in actual calculations. It can also be chosen to be a small number relative to the size of the typical u_i under calculation.

2.2 WENO reconstruction

Comparing with the problem of WENO interpolation described in the previous subsection, the problem of WENO reconstruction is more relevant to numerical solutions of conservation laws. To describe this reconstruction problem, we still use the uniform mesh $x_i = i \Delta x$ and the half points $x_{i+\frac{1}{2}} = \frac{1}{2}(x_i + x_{i+1})$. Instead of assuming that the grid values u_i of the function $u(x)$ are known, we assume that its cell averages

$$\bar{u}_i = \frac{1}{\Delta x} \int_{x_{i-\frac{1}{2}}}^{x_{i+\frac{1}{2}}} u(x) dx$$

over the intervals $I_i = (x_{i-\frac{1}{2}}, x_{i+\frac{1}{2}})$ are given. We would again like to find an approximation of the function $u(x)$ at a given point, for example at the half nodes $x_{i+\frac{1}{2}}$.

Even though this problem looks different from that of interpolation, they are in fact closely related. If we define the primitive function of $u(x)$ by

$$U(x) = \int_{x_{i-\frac{1}{2}}}^x u(\xi) d\xi$$

where the lower limit $x_{-\frac{1}{2}}$ is irrelevant and can be replaced by any fixed point, then we clearly have

$$U(x_{i+\frac{1}{2}}) = \int_{x_{-\frac{1}{2}}}^{x_{i+\frac{1}{2}}} u(\xi) d\xi = \sum_{l=0}^i \int_{x_{l-\frac{1}{2}}}^{x_{l+\frac{1}{2}}} u(\xi) d\xi = \sum_{l=0}^i \Delta x \bar{u}_l$$

That is, with the knowledge of all the cell averages \bar{u}_l , we also have the knowledge of the point values of the primitive function $U(x_{i+\frac{1}{2}})$ at all half nodes. Therefore, interpolation polynomials can be constructed for the primitive function $U(x)$. The derivative of such an interpolation polynomial for $U(x)$ can then be used as an approximation to $u(x) = U'(x)$.

We carry out this procedure for an example similar to the one described in the previous subsection. Let $P_1(x)$ be the polynomial of degree at most three which interpolates the function $U(x)$ at the four points $x_{j+\frac{1}{2}}$, $j = i-3, i-2, i-1, i$, and let $p_1(x) = P'_1(x)$, then it is easy to verify that $p_1(x)$ is the unique polynomial of degree at most two which “reconstructs” the function $u(x)$ over the stencil $S_1 = \{I_{i-2}, I_{i-1}, I_i\}$, in the sense that

$$(\bar{p}_1)_j = \frac{1}{\Delta x} \int_{x_{j-\frac{1}{2}}}^{x_{j+\frac{1}{2}}} p_1(x) dx = \bar{u}_j, \quad j = i-2, i-1, i$$

One could then use $u_{i+\frac{1}{2}}^{(1)} \equiv p_1(x_{i+\frac{1}{2}})$ as an approximation to the value $u(x_{i+\frac{1}{2}})$. A simple algebra leads to the explicit formula for this approximation

$$u_{i+\frac{1}{2}}^{(1)} = \frac{1}{3}\bar{u}_{i-2} - \frac{7}{6}\bar{u}_{i-1} + \frac{11}{6}\bar{u}_i \tag{2.10}$$

From the relationship $p_1(x) = P'_1(x)$ and the elementary numerical analysis about the interpolation polynomial $P_1(x)$, we know that this approximation is third order accurate

$$u_{i+\frac{1}{2}}^{(1)} - u(x_{i+\frac{1}{2}}) = O(\Delta x^3)$$

if the function $u(x)$ is smooth in the stencil S_1 . Similarly, a different stencil $S_2 = \{I_{i-1}, I_i, I_{i+1}\}$ would yield a different reconstruction polynomial $p_2(x)$ satisfying $(\bar{p}_2)_j = \bar{u}_j$ for $j = i-1, i, i+1$, hence a different approximation $u_{i+\frac{1}{2}}^{(2)} \equiv p_2(x_{i+\frac{1}{2}})$ to $u(x_{i+\frac{1}{2}})$, given explicitly as

$$u_{i+\frac{1}{2}}^{(2)} = -\frac{1}{6}\bar{u}_{i-1} + \frac{5}{6}\bar{u}_i + \frac{1}{3}\bar{u}_{i+1} \tag{2.11}$$

which is also third order accurate

$$u_{i+\frac{1}{2}}^{(2)} - u(x_{i+\frac{1}{2}}) = O(\Delta x^3)$$

provided that the function $u(x)$ is smooth in the stencil S_2 . Finally, a third stencil $S_3 = \{I_i, I_{i+1}, I_{i+2}\}$ would lead to a third reconstruction polynomial $p_3(x)$, satisfying $(\bar{p}_3)_j = \bar{u}_j$ for $j = i, i+1, i+2$ and giving another approximation $u_{i+\frac{1}{2}}^{(3)} \equiv p_3(x_{i+\frac{1}{2}})$, or explicitly as

$$u_{i+\frac{1}{2}}^{(3)} = \frac{1}{3}\bar{u}_i + \frac{5}{6}\bar{u}_{i+1} - \frac{1}{6}\bar{u}_{i+2} \quad (2.12)$$

which is of course also third order accurate

$$u_{i+\frac{1}{2}}^{(3)} - u(x_{i+\frac{1}{2}}) = O(\Delta x^3)$$

provided that the function $u(x)$ is smooth in the stencil S_3 .

If we use the large stencil $S = \{I_{i-2}, I_{i-1}, I_i, I_{i+1}, I_{i+2}\}$, which is the union of all three third order stencils S_1 , S_2 and S_3 , then we would be able to obtain a reconstruction polynomial $p(x)$ of degree at most four, satisfying $\bar{p}_j = \bar{u}_j$ for $j = i-2, i-1, i, i+1, i+2$, and giving an approximation $u_{i+\frac{1}{2}} \equiv p(x_{i+\frac{1}{2}})$, or explicitly as

$$u_{i+\frac{1}{2}} = \frac{1}{30}\bar{u}_{i-2} - \frac{13}{60}\bar{u}_{i-1} + \frac{47}{60}\bar{u}_i + \frac{9}{20}\bar{u}_{i+1} - \frac{1}{20}\bar{u}_{i+2} \quad (2.13)$$

which is fifth order accurate

$$u_{i+\frac{1}{2}} - u(x_{i+\frac{1}{2}}) = O(\Delta x^5)$$

provided that the function $u(x)$ is smooth in the large stencil S .

As before, the fifth order approximation $u_{i+\frac{1}{2}}$, defined in (2.13), based on the large stencil S , can be written as a linear convex combination of the three third order approximations $u_{i+\frac{1}{2}}^{(1)}$, $u_{i+\frac{1}{2}}^{(2)}$ and $u_{i+\frac{1}{2}}^{(3)}$, defined by (2.10), (2.11), (2.12) and based on the three small stencils S_1 , S_2 and S_3 respectively:

$$u_{i+\frac{1}{2}} = \gamma_1 u_{i+\frac{1}{2}}^{(1)} + \gamma_2 u_{i+\frac{1}{2}}^{(2)} + \gamma_3 u_{i+\frac{1}{2}}^{(3)} \quad (2.14)$$

where the linear weights γ_1 , γ_2 and γ_3 , satisfying $\gamma_1 + \gamma_2 + \gamma_3 = 1$, are given in this reconstruction case as

$$\gamma_1 = \frac{1}{10}, \quad \gamma_2 = \frac{3}{5}, \quad \gamma_3 = \frac{3}{10}.$$

In the WENO literature, the reconstruction (2.14) is sometimes referred to as a *linear reconstruction*, not because it is a reconstruction using a linear function, but because the weights γ_1 , γ_2 and γ_3 are constant linear weights. The WENO idea is again to choose the final approximation as a convex combination of the three third order approximations

$$u_{i+\frac{1}{2}} = w_1 u_{i+\frac{1}{2}}^{(1)} + w_2 u_{i+\frac{1}{2}}^{(2)} + w_3 u_{i+\frac{1}{2}}^{(3)} \quad (2.15)$$

where the nonlinear weights $w_j \geq 0$ are determined again by (2.9), with the smoothness indicators determined by (2.7). However, since the reconstruction polynomials $p_j(x)$ are different from the interpolation polynomials there, the explicit formulas of the smoothness indicators would change from (2.8) to

$$\begin{aligned} \beta_1 &= \frac{13}{12} (\bar{u}_{i-2} - 2\bar{u}_{i-1} + \bar{u}_i)^2 + \frac{1}{4} (\bar{u}_{i-2} - 4\bar{u}_{i-1} + 3\bar{u}_i)^2 \\ \beta_2 &= \frac{13}{12} (\bar{u}_{i-1} - 2\bar{u}_i + \bar{u}_{i+1})^2 + \frac{1}{4} (\bar{u}_{i-1} - \bar{u}_{i+1})^2 \\ \beta_3 &= \frac{13}{12} (\bar{u}_i - 2\bar{u}_{i+1} + \bar{u}_{i+2})^2 + \frac{1}{4} (3\bar{u}_i - 4\bar{u}_{i+1} + \bar{u}_{i+2})^2 \end{aligned} \quad (2.16)$$

In Figure 2.1, we compare a fifth order WENO reconstruction (left picture) with a fifth order linear reconstruction (2.13) (right picture), to a discontinuous function. We can clearly observe that the linear reconstruction has spurious oscillations near the discontinuity, while the WENO reconstruction is non-oscillatory.

2.3 Further remarks

The WENO interpolation problem discussed in Section 2.1 has been used in [135] to transfer information from one domain to another in a high order, non-oscillatory fashion for a multi-domain WENO scheme. It has also been used in [13] to build a high order Lagrangian type method for solving Hamilton-Jacobi equations. In fact in [13], it is proven that the interpolation polynomial $p(x)$ of degree at most $2k - 1$ over the large stencil, and the interpolation

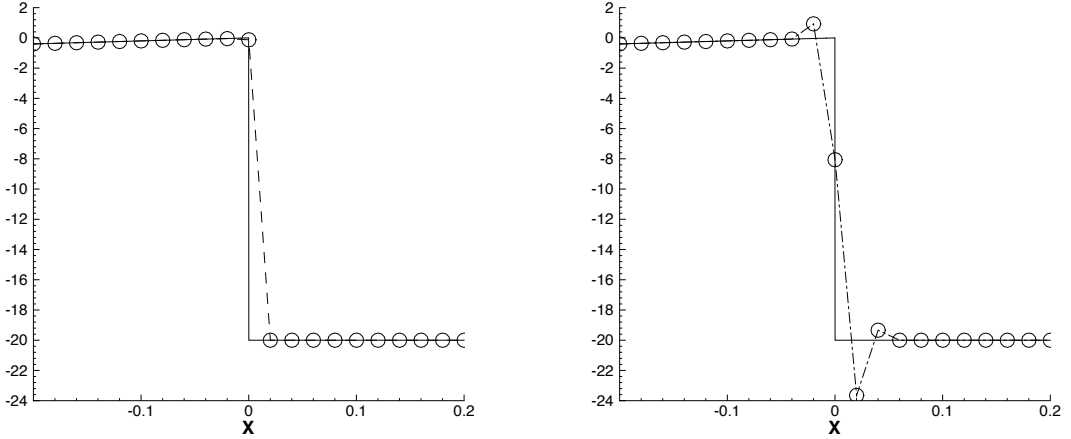


Figure 2.1: Reconstructions to $u(x_{i+1/2})$. Solid lines: exact function; symbols: reconstructed approximations. Left: fifth order WENO reconstruction. Right: fifth order linear weight reconstruction.

polynomials $p_l(x)$ of degree at most k over the k smaller sub-stencils whose union is the large stencil, are related by

$$p(x) = \sum_{l=1}^k \gamma_l(x) p_l(x),$$

where the linear weights $\gamma_l(x)$ are polynomials of degree at most $k-1$ and $\gamma_l(x) \geq 0$ for x in the common interval of all the sub-stencils. By choosing x to be a specific point, e.g. $x = x_{i+\frac{1}{2}}$, we would recover results in Section 2.1.

The WENO reconstruction problem discussed in Section 2.2 is the building block of all WENO schemes for solving hyperbolic conservation laws. The third order version was discussed in the first WENO paper [101]. The fifth order version and the general framework for the smoothness indicator (2.7) were discussed in [76]. Higher order versions of this WENO reconstruction were discussed in [4].

Notice that neither the interpolation problem in Section 2.1 nor the reconstruction problem in Section 2.2 requires uniform or smooth meshes. We have given the presentation using uniform meshes just for simplicity. In applications, e.g. [13, 139], WENO interpolations and reconstructions on non-uniform and non-smooth meshes are used. The procedures are identical to those described in Sections 2.1 and 2.2. The only difference is that the coefficients in,

e.g. (2.1)-(2.4), the linear weights in, e.g. (2.5), and the coefficients in the explicit formulas of the smoothness indicators in, e.g. (2.8), would all become local constants depending on the mesh sizes in the stencil.

Two and three dimensional interpolation and reconstruction in tensor product meshes can be performed in a dimension by dimension fashion, with the one dimensional procedure discussed in the previous subsections used in each dimension. The interpolation and reconstruction procedures can also be generalized to truly multi-dimensional unstructured meshes, for example triangular meshes in 2D and tetrahedral meshes in 3D. However, the details of such generalization are much more involved than the one dimensional version. We refer to, e.g. [183] for the two dimensional WENO interpolation and [71, 184] for the two and three dimensional WENO reconstruction on unstructured meshes.

In some of the WENO interpolation and reconstruction problems, especially in some of the reconstruction problems, one might encounter linear weights γ_j 's in, e.g. (2.5) which are negative. Notice that these linear weights are determined uniquely by the accuracy requirement, hence if they happen to be negative, one must find a way to deal with the difficulty that the linear combination in, e.g. (2.5) is no longer a convex combination. If the usual WENO procedure is used without modification, oscillations and instability may appear. This is because a sum of monotone approximations with negative linear weights may become non-monotone, even though the linear weights sum to one. A procedure to systematically modify the WENO procedure so that it is still stable and non-oscillatory in the presence of negative weights is developed in [139] and has been used in many later works, such as in [124] where this technique is used to construct high order central WENO schemes, in [120] where it is used to construct high order staggered finite difference WENO schemes, in [17] where it is used to construct high order WENO schemes for solving non-conservative hyperbolic systems, and in [110, 163, 164] where it is used to construct well-balanced high order WENO schemes for a class of balance laws including the shallow water equations. In Figure 2.2 we give an example of using WENO schemes on general triangulations [71] to

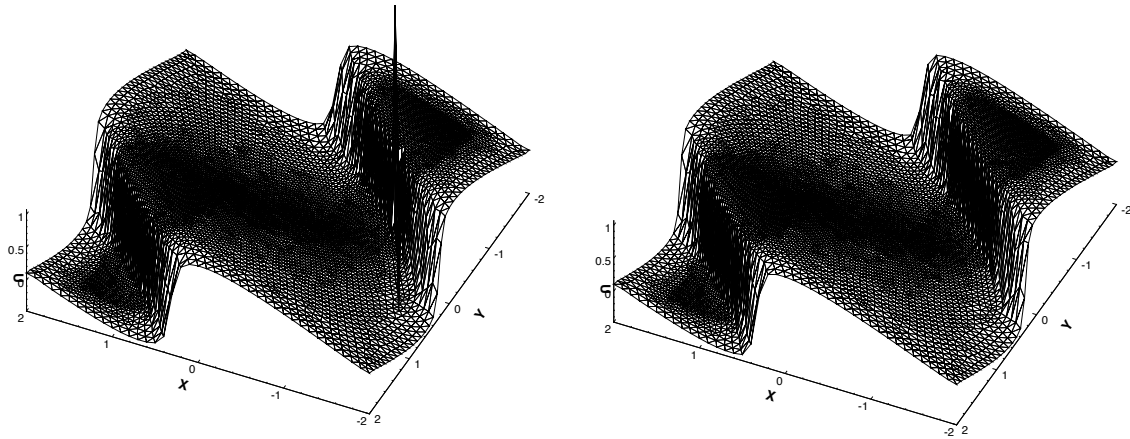


Figure 2.2: Fourth order WENO scheme [71] solving the two-dimensional Burgers equation on a unstructured triangular mesh. Left: without any special treatment for the negative linear weights. Right: with the special treatment for the negative linear weights in [139].

solve the nonlinear Burgers equation in two-dimensions, where negative linear weights do appear, without any modification (left picture) and with the modification designed in [139] (right picture). Clearly, for this example, the scheme is not stable without modification in the presence of negative linear weights, and it is stable with the modification in [139].

Another approach to avoid the appearance of negative linear weights is to lower the accuracy requirement for the linear combination in, e.g. (2.5). For example, if we do not insist that $u_{i+\frac{1}{2}}$ in (2.5) achieves the maximum fifth order accuracy, but require it to be only fourth order accurate, then we have a free parameter in the determination of the linear weights γ_j 's. We can then explore this freedom to make all the linear weights positive. In the extreme case, we could require $u_{i+\frac{1}{2}}$ in (2.5) to be only third order accurate, namely it is no more accurate than the approximation in each sub-stencil. In this case *any* linear weights satisfying $\sum_j \gamma_j = 1$ would be fine. One could then for example take all the γ_j to be equal and positive, or choose the γ_j corresponding to the most symmetric sub-stencil to be the largest. The drawback of this approach is of course a loss in accuracy: with the same large stencil, WENO schemes designed in this approach have a lower order accuracy than the “authentic” WENO schemes described in previous subsections. In [88], this technique

is used to construct high order central WENO schemes, and in [48, 42, 43] it is used to construct finite volume WENO schemes on unstructured meshes.

Besides the interpolation and reconstruction problems discussed in Sections 2.1 and 2.2, there are also many other problems in which a similar WENO procedure can be designed. Two of such examples include:

1. Approximation to the derivative of a given function $u(x)$, given its point values $u_i = u(x_i)$. The procedure is similar to the interpolation problem in Section 2.1: one would first find interpolation polynomials $P_j(x)$ in the sub-stencils and $P(x)$ in the large stencil, then one would find the linear weights γ_j so that

$$P'(x_i) = \sum_j \gamma_j P'_j(x_i)$$

if we would need the approximation of the derivative at $x = x_i$. The remaining procedure is similar to those in Section 2.1, except that the smoothness indicator (2.7) should be replaced by

$$\beta_j = \sum_{l=2}^k \Delta x^{2l-1} \int_{x_{i-\frac{1}{2}}}^{x_{i+\frac{1}{2}}} \left(\frac{d^l}{dx^l} P_j(x) \right)^2 dx.$$

This is because $P'_j(x)$ are our building blocks, hence the measurement of their smoothness should start from the second derivative of $P_j(x)$. This WENO derivative procedure is used in the design of WENO schemes for the Hamilton-Jacobi equations [75]. It is in fact also indirectly used in the WENO reconstruction procedure described in Section 2.2 on the primitive function $U(x)$.

Clearly, one could also design similar WENO procedures to approximate the second or higher order derivatives of $u(x)$.

2. Approximations to the integral of a given function $u(x)$, given its point values $u_i = u(x_i)$. The procedure is parallel to the interpolation procedure described in Section 2.1. For example, we could use the integral $I_i^{(1)} = \int_{x_{i-\frac{1}{2}}}^{x_{i+\frac{1}{2}}} p_1(x) dx$ of the unique polynomial

$p_1(x)$ of degree at most two, which interpolates the function $u(x)$ at the mesh points in the stencil $S_1 = \{x_{i-2}, x_{i-1}, x_i\}$, to approximate the integral $\int_{x_{i-\frac{1}{2}}}^{x_{i+\frac{1}{2}}} u(x)dx$. A simple algebra leads to the explicit formula for this approximation:

$$I_i^{(1)} = \Delta x \left(\frac{1}{24}u_{i-2} - \frac{1}{12}u_{i-1} + \frac{25}{24}u_i \right) \quad (2.17)$$

From elementary numerical analysis, we know that this approximation is fourth order accurate

$$I_i^{(1)} - \int_{x_{i-\frac{1}{2}}}^{x_{i+\frac{1}{2}}} u(x)dx = O(\Delta x^4)$$

if the function $u(x)$ is smooth in the stencil S_1 . Similarly, one obtains the approximations $I_i^{(2)}$ and $I_i^{(3)}$ based on the interpolation polynomials $p_2(x)$ and $p_3(x)$ over the stencils $S_2 = \{x_{i-1}, x_i, x_{i+1}\}$ and $S_3 = \{x_i, x_{i+1}, x_{i+2}\}$ respectively, explicitly given as

$$I_i^{(2)} = \Delta x \left(\frac{1}{24}u_{i-1} + \frac{11}{12}u_i + \frac{1}{24}u_{i+1} \right) \quad (2.18)$$

and

$$I_i^{(3)} = \Delta x \left(\frac{25}{24}u_i - \frac{1}{12}u_{i+1} + \frac{1}{24}u_{i+2} \right). \quad (2.19)$$

$I_i^{(2)}$ or $I_i^{(3)}$ is a fourth order accurate approximation to $\int_{x_{i-\frac{1}{2}}}^{x_{i+\frac{1}{2}}} u(x)dx$ if the function $u(x)$ is smooth in the relevant stencil S_2 or S_3 . Finally, the approximation I_i based on the interpolating polynomial $p(x)$ over the large stencil $S = \{x_{i-2}, x_{i-1}, x_i, x_{i+1}, x_{i+2}\}$, explicitly given as

$$I_i = \Delta x \left(-\frac{17}{5760}u_{i-2} + \frac{77}{1440}u_{i-1} + \frac{863}{960}u_i + \frac{77}{1440}u_{i+1} - \frac{17}{5760}u_{i+2} \right), \quad (2.20)$$

is a sixth order approximation to $\int_{x_{i-\frac{1}{2}}}^{x_{i+\frac{1}{2}}} u(x)dx$ if the function $u(x)$ is smooth in the large stencil S . As before, this sixth order approximation I_i can be written as a linear combination of the three fourth order approximations $I_i^{(1)}$, $I_i^{(2)}$ and $I_i^{(3)}$:

$$I_i = \gamma_1 I_i^{(1)} + \gamma_2 I_i^{(2)} + \gamma_3 I_i^{(3)} \quad (2.21)$$

where the linear weights γ_1 , γ_2 and γ_3 are given in this case as

$$\gamma_1 = -\frac{17}{240}, \quad \gamma_2 = \frac{137}{120}, \quad \gamma_3 = -\frac{17}{240}.$$

Notice that this time some of the linear weights are negative. The remaining WENO procedure is similar to those in Section 2.1, except that we would need to use the technique in [139] to handle the negative linear weights. The smoothness indicators are again given by (2.7) or explicitly by (2.8).

This WENO integration procedure is used in the design of high order residual distribution conservative finite difference WENO schemes in [24, 25].

Finally, we mention that the choice of the nonlinear weights (2.9) is not unique. For example, [68] discusses another choice of the nonlinear weights, based on the same smoothness indicators (2.7), to enhance accuracy in smooth regions, especially at smooth extrema. The choice of the smoothness indicators (2.7) is also not unique. For example, [178] discusses another choice of the smoothness indicators to obtain better convergence to steady states of the WENO schemes for one and two dimensional nonlinear hyperbolic systems.

3 WENO schemes for hyperbolic conservation laws

The main application of the WENO procedure is in solving hyperbolic conservation laws

$$u_t + f(u)_x = 0. \quad (3.1)$$

A conservation law could be as simple as a one dimensional scalar equation (3.1) or as complicated as a three-dimensional system

$$u_t + f(u)_x + g(u)_y + h(u)_z = 0 \quad (3.2)$$

where u is a vector and any linear combination of the Jacobians $\xi_1 f'(u) + \xi_2 g'(u) + \xi_3 h'(u)$ for real ξ_1 , ξ_2 and ξ_3 must have only real eigenvalues and a complete set of independent eigenvectors. We will mostly use the simple one dimensional scalar equation (3.1) to describe the ideas of various WENO schemes. We will mention the generalizations to multi-dimensional problems in Section 3.4 and to systems in Section 3.5.

3.1 Finite volume schemes

A finite volume scheme approximates the conservation law (3.1) in its integral form

$$\frac{d}{dt}\bar{u}_i + \frac{1}{\Delta x_i} \left(f(u_{i+\frac{1}{2}}) - f(u_{i-\frac{1}{2}}) \right) = 0 \quad (3.3)$$

where $\bar{u}_i = \frac{1}{\Delta x} \int_{x_{i-\frac{1}{2}}}^{x_{i+\frac{1}{2}}} u(x, t) dx$ is the spatial cell average of the solution $u(x, t)$ in the cell $I_i = (x_{i-\frac{1}{2}}, x_{i+\frac{1}{2}})$ as defined in Section 2.2.

To convert (3.3) to a finite volume scheme, we take our computational variables as the cell averages $\{\bar{u}_i\}$ and use the WENO reconstruction procedure described in Section 2.2 to obtain an approximation to $u_{i+\frac{1}{2}}$. An additional complication is that the solution to the conservation law (3.1) follows characteristics, hence a stable numerical scheme should also propagate its information in the same characteristic direction, which is referred to as *upwinding*. This is achieved by replacing $f(u_{i+\frac{1}{2}})$ by

$$\hat{f} \left(u_{i+\frac{1}{2}}^-, u_{i+\frac{1}{2}}^+ \right)$$

where $\hat{f}(u^-, u^+)$ is a monotone numerical flux satisfying

- $\hat{f}(u^-, u^+)$ is non-decreasing in its first argument u^- and non-increasing in its second argument u^+ , symbolically $\hat{f}(\uparrow, \downarrow)$;
- $\hat{f}(u^-, u^+)$ is consistent with the physical flux $f(u)$, i.e. $\hat{f}(u, u) = f(u)$;
- $\hat{f}(u^-, u^+)$ is Lipschitz continuous with respect to both arguments u^- and u^+ .

Examples of monotone fluxes include

- The Godunov flux

$$\hat{f}^{God}(u^-, u^+) = \begin{cases} \min_{u^- \leq u \leq u^+} f(u), & \text{if } u^- \leq u^+; \\ \max_{u^+ \leq u \leq u^-} f(u), & \text{if } u^- > u^+ \end{cases}$$

- The Lax-Friedrichs flux

$$\hat{f}^{LF}(u^-, u^+) = \frac{1}{2} \left(f(u^-) + f(u^+) - \alpha(u^+ - u^-) \right)$$

where $\alpha = \max_u |f'(u)|$

- The Engquist-Osher flux

$$\hat{f}^{LF}(u^-, u^+) = f^+(u^-) + f^-(u^+)$$

where

$$f^+(u) = f(0) + \int_0^u \max(f'(v), 0) dv;$$

$$f^-(u) = \int_0^u \min(f'(v), 0) dv$$

etc. We refer to, e.g. [86] and references therein for a detailed discussion of monotone fluxes.

The approximations $u_{i+\frac{1}{2}}^-$ and $u_{i+\frac{1}{2}}^+$ are the WENO reconstructions from stencils one point biased to the left and one point biased to the right, respectively. For example, for a fifth order WENO scheme, the reconstruction $u_{i+\frac{1}{2}}^-$ uses the following 5-cell stencil

$$I_{i-2}, I_{i-1}, I_i, I_{i+1}, I_{i+2}$$

and the reconstruction $u_{i+\frac{1}{2}}^+$ uses the following 5-cell stencil

$$I_{i-1}, I_i, I_{i+1}, I_{i+2}, I_{i+3}.$$

The details of these WENO reconstructions have already been given in Section 2.2.

The finite volume scheme described above can be written as a method-of-lines ordinary differential equation (ODE) system

$$\frac{d}{dt}\bar{u}_i = -\frac{1}{\Delta x} \left[\hat{f} \left(u_{i+\frac{1}{2}}^-, u_{i+\frac{1}{2}}^+ \right) - \hat{f} \left(u_{i-\frac{1}{2}}^-, u_{i-\frac{1}{2}}^+ \right) \right] \equiv L(\bar{u})_i \quad (3.4)$$

This ODE system can be discretized in time by the total variation diminishing (TVD) Runge-Kutta time discretization methods [146], which is also known as the strong stability preserving (SSP) methods [56]. A good property of such time discretization techniques is that it maintains stability in the total variation semi-norm, or any other norm or semi-norm, of the first order Euler forward method with the same spatial discretization. The most popular TVD Runge-Kutta time discretization method is the third order accurate version

in [146]:

$$\begin{aligned}\bar{u}^{(1)} &= \bar{u}^n + \Delta t L(\bar{u}^n) \\ \bar{u}^{(2)} &= \frac{3}{4} \bar{u}^n + \frac{1}{4} \bar{u}^{(1)} + \frac{1}{4} \Delta t L(\bar{u}^{(1)}) \\ \bar{u}^{n+1} &= \frac{1}{3} \bar{u}^n + \frac{2}{3} \bar{u}^{(2)} + \frac{2}{3} \Delta t L(\bar{u}^{(2)})\end{aligned}\tag{3.5}$$

Such time discretizations are also used for the finite difference schemes discussed below. Multi-step methods having this stability property are also available [141]. An alternative method of time discretization is via the Lax-Wendroff procedure, namely performing a Taylor expansion in time and converting all time derivatives to spatial derivatives by repeatedly using the PDE, and finally discretizing all the spatial derivatives to the correct order of accuracy. See, e.g. [155, 125].

3.2 Finite difference schemes

A finite difference scheme approximates the conservation law (3.1) directly. The computational variables are the point values $\{u_i\}$ of the solution, and the scheme is required to be in conservation form

$$\frac{d}{dt} u_i + \frac{1}{\Delta x} \left(\hat{f}_{i+\frac{1}{2}} - \hat{f}_{i-\frac{1}{2}} \right) = 0 \tag{3.6}$$

where the numerical flux

$$\hat{f}_{i+\frac{1}{2}} = \hat{f}(u_{i-p}, \dots, u_{i+q}) \tag{3.7}$$

is consistent with the physical flux $\hat{f}(u, \dots, u) = f(u)$ and is Lipschitz continuous with respect to all its arguments.

The scheme is r -th order accurate if

$$\frac{1}{\Delta x} \left(\hat{f}_{i+\frac{1}{2}} - \hat{f}_{i-\frac{1}{2}} \right) = f(u)_x|_{x=x_i} + O(\Delta x^r)$$

when u is smooth in the stencil.

It seems that finite difference schemes are conceptually very different from finite volume schemes. However, the following simple lemma by Shu and Osher [147] establishes the relationship between the finite volume and finite difference schemes.

Lemma 3.1: If $h(x) = h_{\Delta x}(x)$ is implicitly defined as

$$\frac{1}{\Delta x} \int_{x-\frac{\Delta x}{2}}^{x+\frac{\Delta x}{2}} h(\xi) d\xi = f(u(x)) \quad (3.8)$$

then

$$\frac{1}{\Delta x} \left(h(x_{i+\frac{1}{2}}) - h(x_{i-\frac{1}{2}}) \right) = f(u)_x|_{x=x_i}.$$

The proof is straightforward: just take a x derivative on both sides of (3.8).

This simple lemma indicates that we can take the numerical flux in the finite difference scheme as

$$\hat{f}_{i+\frac{1}{2}} = h(x_{i+\frac{1}{2}}) \quad (3.9)$$

to ensure r -th order accuracy, if the function $h(x)$ in the Lemma can be computed to r -th order accuracy.

In fact, the (implicit) definition (3.8) of $h(x)$ implies that

$$\bar{h}_i \equiv \frac{1}{\Delta x} \int_{x_{i-\frac{1}{2}}}^{x_{i+\frac{1}{2}}} h(\xi) d\xi = f(u_i)$$

is known for a finite difference scheme, since the point values u_i are the computational variables. Therefore, we are given the cell averages \bar{h}_i of the function $h(x)$ and we would need to approximate its point values $h(x_{i+\frac{1}{2}})$ to high order accuracy to obtain the numerical flux $\hat{f}_{i+\frac{1}{2}}$ in (3.9). Hence we can use the same WENO reconstruction procedure discussed in Section 2.2 which has been used for finite volume schemes! This implies that a finite difference WENO code for the scalar one dimensional conservation law (3.1) shares the main reconstruction subroutine with a finite volume WENO code. The only difference is the input-output pair: for a finite volume scheme, the input is the set of cell averages $\{\bar{u}_i\}$ and the output is the reconstructed values of the solution at the cell interfaces $\{u_{i+\frac{1}{2}}\}$; for a finite difference scheme, the input is the set of the point values of the physical flux $\{f(u_i)\}$ and the output is the numerical fluxes at the cell interfaces $\{\hat{f}_{i+\frac{1}{2}}\}$.

For the purpose of stability, the finite difference procedure described above is applied to $f^+(u)$ and $f^-(u)$ separately, where $f^\pm(u)$ correspond to a flux splitting

$$f(u) = f^+(u) + f^-(u) \quad (3.10)$$

with

$$\frac{d}{du} f^+(u) \geq 0, \quad \frac{d}{du} f^-(u) \leq 0. \quad (3.11)$$

The reconstruction for $f^+(u)$ uses a biased stencil with one more point to the left, and that for $f^-(u)$ uses a biased stencil with one more point to the right, to obey correct upwinding. We further require that $f^\pm(u)$ are as smooth functions of u as $f(u)$. The most commonly used flux splitting is the Lax-Friedrichs splitting

$$f^\pm(u) = \frac{1}{2} (f(u) \pm \alpha u)$$

with

$$\alpha = \max_u |f'(u)|.$$

However, other splittings can also be used. See, e.g. [76]. Notice that for any flux splitting (3.10) satisfying (3.11), $\hat{f}(u^-, u^+) = f^+(u^-) + f^-(u^+)$ is a monotone flux.

Finally, we remark that the finite difference WENO scheme discussed in this section can only be used on uniform or smooth meshes. Superficially, this is because Lemma 3.1 does not hold if Δx is not a constant. A deeper reason is given in [106]. A conservative finite difference scheme (3.6) with a local flux (3.7) cannot achieve higher than second order accuracy on arbitrary non-uniform non-smooth meshes.

3.3 Comparison of finite volume and finite difference schemes

We can now summarize the main features of the finite volume and the finite difference WENO schemes for solving the scalar one dimensional conservation law (3.1) as follows.

- A finite volume WENO scheme

1. is based on the cell averages $\{\bar{u}_i\}$ and uses the integral form (3.3) of the PDE;

- 2. needs a WENO reconstruction described in Section 2.2 with the cell averages $\{\bar{u}_i\}$ as input and with the reconstructed point values $\{u_{i+1/2}^\pm\}$ as output;
 - 3. can use any monotone flux $\hat{f}(u^-, u^+)$;
 - 4. can be applied to any meshes and does not need uniformity or smoothness of the meshes.
- A finite difference WENO scheme
 - 1. is based on the point values $\{u_i\}$, and uses the original PDE form (3.1) directly;
 - 2. needs a WENO reconstruction described in Section 2.2 with the point values of the split fluxes $\{f^\pm(u_i)\}$ as input and with the numerical fluxes $\{\hat{f}_{i+1/2}^\pm\}$ as output;
 - 3. can only use monotone fluxes which correspond to smooth flux splitting $f(u) = f^+(u) + f^-(u)$ satisfying (3.11);
 - 4. can only be applied to uniform or smooth meshes.

Based on this comparison, we conclude that, for solving the one dimensional scalar conservation law (3.1), the cost of the finite volume and the finite difference WENO schemes is the same (in fact they both involve the same WENO reconstruction procedure, the only difference is the input-output pair). The finite volume scheme is more flexible in its applicability to any monotone fluxes and to any non-uniform non-smooth meshes. It would seem that the finite volume scheme is clearly the winner. This conclusion is valid for all one dimensional calculations, including the case of one dimensional systems. However, as we will see in next subsection, the conclusion of this comparison changes dramatically for multi-dimensional problems.

3.4 Multi-dimensional problems

We use a two dimensional scalar conservation law

$$u_t + f(u)_x + g(u)_y = 0 \quad (3.12)$$

to demonstrate finite volume and finite difference WENO schemes for multi-dimensional problems. Furthermore, we assume that we have a tensor product mesh which is uniform in both x and y . If we integrate the PDE (3.12) over a typical cell $I_{ij} \equiv [x_{i-\frac{1}{2}}, x_{i+\frac{1}{2}}] \times [y_{j-\frac{1}{2}}, y_{j+\frac{1}{2}}]$, we obtain the integral form

$$\begin{aligned} \frac{d\tilde{u}_{ij}(t)}{dt} &= -\frac{1}{\Delta x \Delta y} \left(\int_{y_{j-\frac{1}{2}}}^{y_{j+\frac{1}{2}}} f(u(x_{i+\frac{1}{2}}, y, t)) dy - \int_{y_{j-\frac{1}{2}}}^{y_{j+\frac{1}{2}}} f(u(x_{i-\frac{1}{2}}, y, t)) dy \right. \\ &\quad \left. + \int_{x_{i-\frac{1}{2}}}^{x_{i+\frac{1}{2}}} g(u(x, y_{j+\frac{1}{2}}, t)) dx - \int_{x_{i-\frac{1}{2}}}^{x_{i+\frac{1}{2}}} g(u(x, y_{j-\frac{1}{2}}, t)) dx \right) \end{aligned} \quad (3.13)$$

where \tilde{u} is the cell average

$$\tilde{u}_{ij}(t) \equiv \frac{1}{\Delta x \Delta y} \int_{y_{j-\frac{1}{2}}}^{y_{j+\frac{1}{2}}} \int_{x_{i-\frac{1}{2}}}^{x_{i+\frac{1}{2}}} u(x, y, t) dx dy$$

In particular, our notation is that \bar{v} stands for the cell average in x :

$$\bar{v}_{ij} = \frac{1}{\Delta x} \int_{x_{i-\frac{1}{2}}}^{x_{i+\frac{1}{2}}} v(x, y_j) dx$$

and \tilde{v} stands for the cell average in y :

$$\tilde{v}_{ij} = \frac{1}{\Delta y} \int_{y_{j-\frac{1}{2}}}^{y_{j+\frac{1}{2}}} v(x_i, y) dy$$

We approximate the integral form (3.13) by a finite volume scheme

$$\frac{d\tilde{u}_{ij}(t)}{dt} = -\frac{1}{\Delta x} (\hat{f}_{i+\frac{1}{2},j} - \hat{f}_{i-\frac{1}{2},j}) - \frac{1}{\Delta y} (\hat{g}_{i,j+\frac{1}{2}} - \hat{g}_{i,j-\frac{1}{2}})$$

where the numerical fluxes are given by

$$\begin{aligned} \hat{f}_{i+\frac{1}{2},j} &\approx -\frac{1}{\Delta y} \int_{y_{j-\frac{1}{2}}}^{y_{j+\frac{1}{2}}} f(u(x_{i+\frac{1}{2}}, y, t)) dy \equiv \tilde{f}_{i+\frac{1}{2},j} \\ \hat{g}_{i,j+\frac{1}{2}} &\approx -\frac{1}{\Delta x} \int_{x_{i-\frac{1}{2}}}^{x_{i+\frac{1}{2}}} g(u(x, y_{j+\frac{1}{2}}, t)) dx \equiv \bar{g}_{i,j+\frac{1}{2}} \end{aligned}$$

First, we look at the simple, linear constant coefficient case

$$u_t + au_x + bu_y = 0$$

we would have

$$\hat{f}_{i+\frac{1}{2},j} = a\tilde{u}_{i+\frac{1}{2},j}, \quad \hat{g}_{i,j+\frac{1}{2}} = b\bar{u}_{i,j+\frac{1}{2}}$$

Therefore we would only need to perform two one-dimensional WENO reconstructions

$$\{\tilde{u}_{ij}\} \rightarrow \{\tilde{u}_{i+\frac{1}{2},j}\} \quad \text{for fixed } j$$

and

$$\{\tilde{u}_{ij}\} \rightarrow \{\bar{u}_{i,j+\frac{1}{2}}\} \quad \text{for fixed } i$$

and the cost is the same as in the one-dimensional case per cell per direction.

However, if the PDE (3.12) is nonlinear, namely if $f(u)$ and $g(u)$ are nonlinear functions of u , then $f(\tilde{u}) \neq \widetilde{f(u)}$, hence we would need to perform two one-dimensional WENO reconstructions and one numerical integration (typically via Gauss quadratures of sufficient accuracy, which bears about the same cost as a reconstruction) to obtain the numerical flux $\hat{f}_{i+\frac{1}{2},j}$. Thus we would need to do

$$\{\tilde{u}_{ij}\} \rightarrow \{\tilde{u}_{i+\frac{1}{2},j}\} \rightarrow \{u_{i+\frac{1}{2},j+j_\alpha}\}_{\alpha=1}^{\alpha_g} \rightarrow \{\hat{f}_{i+\frac{1}{2},j}\}$$

where $\{j + j_\alpha\}_{\alpha=1}^{\alpha_g}$ are the Gaussian quadrature points for the interval $[y_{j-\frac{1}{2}}, y_{j+\frac{1}{2}}]$ with sufficiently high order of accuracy. Likewise for $\hat{g}_{i,j+\frac{1}{2}}$. This is now about three times the cost of the one-dimensional case per cell per direction. The situation will be much worse for three dimensions.

On the other hand, a finite difference scheme approximates the PDE form (3.12) directly and can proceed dimension by dimension. The scheme is

$$\frac{du_{ij}(t)}{dt} = -\frac{1}{\Delta x}(\hat{f}_{i+\frac{1}{2},j} - \hat{f}_{i-\frac{1}{2},j}) - \frac{1}{\Delta y}(\hat{g}_{i,j+\frac{1}{2}} - \hat{g}_{i,j-\frac{1}{2}})$$

where the numerical flux $\hat{f}_{i+\frac{1}{2},j}$ can be computed from $\{u_{ij}\}$ with fixed j in exactly the same way as in the one dimensional case described in Section 3.2. Likewise for $\hat{g}_{i,j+\frac{1}{2}}$. Therefore, the computational cost is exactly the same as in the one-dimensional case per point per direction.

We can now conclude that in 2D, a finite volume scheme (of order of accuracy higher than 2) is 2 to 5 times as expensive as a finite difference scheme of the same order of accuracy using the same mesh and the same reconstruction procedure, depending on specific coding and type of computers. This discrepancy in cost is even bigger for three dimensions. We refer to [18] for a detailed comparison of multi-dimensional finite volume and finite difference schemes in the context of ENO reconstructions. Notice that this difference between finite volume and finite difference schemes is meaningful only for schemes of at least third order accuracy. For first and second order schemes there is no need to distinguish between a finite volume scheme and a finite difference scheme, since the cell average agrees with the value of the function at the cell centroid to second order accuracy.

We should also mention again that finite volume schemes are more flexible than finite difference schemes in terms of monotone fluxes and meshes. Conservative finite volume schemes can be designed on arbitrary meshes. This is a more significant advantage in multi-dimensions as one can design finite volume schemes on unstructured triangulations. However, because of the significant cost advantage, conservative finite difference WENO schemes would be preferable whenever the problem allows a uniform Cartesian or a smooth curvilinear mesh.

3.5 Further remarks

It should be remarked that the WENO reconstruction procedure, when the small parameter ε in (2.9) is chosen to be a small percentage of the size of typical u_i under calculation, is scale invariant. That is, the reconstruction does not change when the solution is amplified by a constant, or when the mesh size Δx changes. The WENO finite volume and finite difference schemes are self-similar, that is, the numerical solution does not change if both the spatial mesh size Δx and the temporal mesh size Δt change by the same factor and $\lambda = \frac{\Delta t}{\Delta x}$ does not change. Since the schemes are self-similar, we do not rely on explicit, mesh size Δx dependent thresholds to determine whether there are discontinuities in the solution and their location. The numerical procedure automatically captures and handles

discontinuities or sharp gradient regions when they appear, so that accuracy and stability are maintained. It is very important to have the numerical schemes satisfying these scale invariant and self-similar properties for many applications.

Since WENO schemes have smooth numerical fluxes and are dissipative, they can be shown to converge with high order accuracy using Strang's framework [150] when the solution of the PDE is smooth [76]. When the solution of the PDE becomes discontinuous, there is no general proof of stability and convergence for high order WENO schemes solving conservation laws. However, in applications WENO schemes perform well in stability and resolution. As to numerically observed order of accuracy in smooth regions of a discontinuous solution, for scalar problems the full designed order of accuracy of the WENO scheme is achieved if we measure the error away from the discontinuity. For systems, because characteristics belonging to different fields than that of the discontinuity may cross the discontinuity and carry the numerical error at the discontinuity into smooth regions, point-wise errors in smooth regions of a high order WENO scheme may fail to achieve the designed order of accuracy, unless a sub-cell resolution technique [62] is used in the shocked cell. We demonstrate this phenomenon by a nozzle flow simulation using a fourth order residual distribution WENO scheme in [24]. In Figure 3.1, we observe good resolution of the WENO numerical solution in comparison with the exact solution of the nonlinear Euler system with source terms. In Table 3.1, we observe that the designed fourth order accuracy is achieved for both upstream and downstream of the shock if a sub-cell integration technique is applied in the shocked cell, while the accuracy downstream of the shock has lower than the designed fourth order accuracy if no special treatment is performed in the shocked cell. Nevertheless, even if the order of accuracy for the pointwise errors downstream of the shock may degenerate for a higher order WENO scheme, the magnitude of the errors is typically still much smaller than that of a lower order scheme on the same mesh. In practice, this is the advantage that we rely on when we use high order WENO schemes to solve complicated nonlinear systems with both shocks and smooth structures in the solutions.

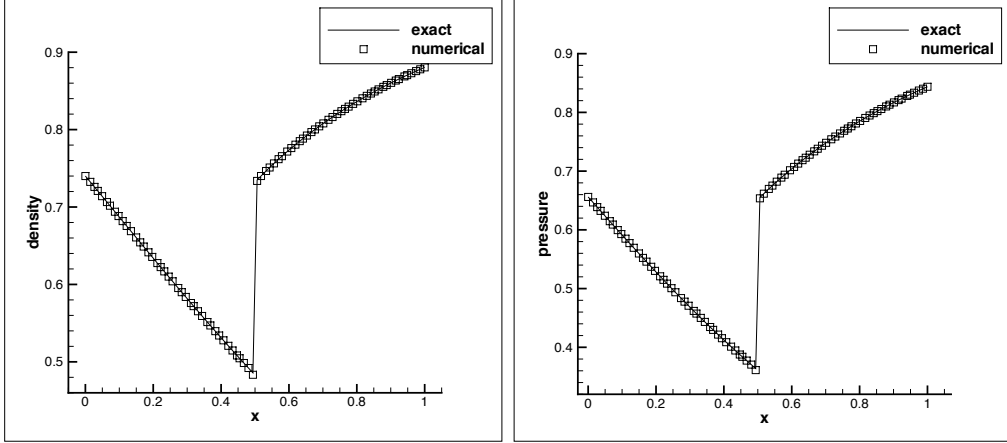


Figure 3.1: Fourth order residual distribution WENO scheme for the nozzle flow problem. Non-smooth mesh with 81 cells. Solid lines: exact solution; symbols: numerical solution. Left: density. Right: pressure.

Even though the pointwise errors for a high order scheme solving discontinuous solutions of a hyperbolic system may show a low order of accuracy, it is well known [83, 103] that the designed high order accuracy is maintained in integrated quantities of the numerical solution such as moments against smooth functions, if the scheme and the PDE are both linear. With this information, we can post-process the numerical solution to obtain the designed order of accuracy also for point values [52]. This is a strong theoretical justification to use high order schemes even for discontinuous solutions. Recently, [54] has given numerical evidence to indicate that such high order information may also be available for high order WENO schemes in solving *nonlinear* systems.

For systems of conservation laws, the WENO schemes have the same structure as those for the scalar cases discussed in the previous subsections. A monotone flux is replaced by an exact or approximate Riemann solver, see, e.g. [156]. The WENO reconstruction can be performed either component-wise, or in local characteristic directions. Usually, component-wise reconstruction produces satisfactory results for schemes up to third order accuracy, while characteristic reconstruction produces better non-oscillatory results for higher order accuracy, albeit with an increased computational cost. Details about the local characteristic

Table 3.1: Fourth order residual distribution WENO scheme for the nozzle flow problem. Errors outside three cells around the shock and numerical orders of accuracy for the density ρ on non-smooth meshes with N cells.

sub-cell separate integrations in the shocked cell								
N	before shock				after shock			
	L^1 error	order	L^∞ error	order	L^1 error	order	L^∞ error	order
21	1.36E-07	-	7.09E-07	-	7.58E-06	-	3.35E-05	-
41	1.44E-08	3.23	6.13E-08	3.53	5.08E-07	3.90	2.19E-06	3.93
81	1.28E-09	3.49	4.85E-09	3.66	1.67E-08	4.93	6.61E-08	5.05
161	8.34E-11	3.94	3.11E-10	3.96	7.72E-10	4.43	3.00E-09	4.46
321	5.41E-12	3.95	2.00E-11	3.96	3.65E-11	4.40	1.36E-10	4.46
641	2.22E-13	4.60	1.20E-12	4.05	1.75E-12	4.38	4.92E-12	4.80
regular integration in the shocked cell								
N	before shock				after shock			
	L^1 error	order	L^∞ error	order	L^1 error	order	L^∞ error	order
21	1.36E-07	-	7.09E-07	-	1.75E-05	-	6.42E-05	-
41	1.44E-08	3.24	6.13E-08	3.53	4.38E-06	1.99	1.42E-05	2.18
81	1.28E-09	3.49	4.85E-09	3.66	1.11E-06	1.98	3.37E-06	2.07
161	8.34E-11	3.94	3.11E-10	3.96	2.34E-07	2.25	7.29E-07	2.21
321	5.41E-12	3.95	2.00E-11	3.96	5.81E-08	2.01	1.77E-07	2.04
641	2.22E-13	4.61	1.22E-12	4.04	8.15E-09	2.83	2.52E-08	2.81

decomposition procedure can be found in many papers, e.g. [64, 146, 148].

When designing numerical schemes to solve hyperbolic systems with source terms

$$u_t + f(u)_x = g(u, x), \quad (3.14)$$

which are also called balance laws, it is a challenge to have the scheme maintaining specific equilibria, that is, steady state solutions satisfying

$$f(u)_x = g(u, x)$$

exactly. This is because such equilibria are usually not constant or polynomial functions, so the truncation error of most schemes will not be exactly zero for such equilibria. A scheme which can maintain such equilibria is referred to as a *well balanced* scheme. The main advantage of well balanced schemes, especially when they are also high order accurate for non-equilibrium solutions of (3.14), is that they can be used to resolve small perturbations

of such equilibria, such as the small amplitude water waves from still water, very accurately without an excessively refined mesh. High order finite difference and finite volume WENO schemes which are well balanced for the still water solution of the shallow water equations, and a more general class of balance laws, are designed in [110, 158, 161, 162, 163, 164]. High order well balanced finite difference WENO schemes for solving the hyperbolic models for chemosensitive movement are designed in [46]. High order finite volume WENO schemes which are well balanced for the moving steady water of the shallow water equations, which are much more difficult to construct, are designed in [111]. As an example, in Figure 3.2 we plot the water surface from a small perturbation (the perturbation amplitude is 1% of the still water height) for later time, simulated by a fifth order well balanced WENO scheme [161]. We can see clearly that the detailed structure of the evolution of such a small perturbation is resolved well even with the relatively coarse mesh of 200×100 points. If a regular, non-well balanced WENO scheme is used, much smaller mesh sizes are needed to resolve the evolution of such small perturbations.

In [136], a modification to the fifth order WENO scheme, termed power WENO scheme, is developed based on an extended class of limiters. Comparison with the standard WENO scheme is made with extensive numerical examples.

In our previous discussion, we have not paid attention to boundary conditions and have assumed the problem has no boundary (compactly supported data or periodic boundary conditions). In practice, of course we would need to deal with various physical boundary conditions. WENO schemes have been used for problems with different boundary conditions such as reflective (solid wall), symmetry (such as the axis in an axis-symmetric setting), inflow and outflow types. A general strategy is to define accurate ghost point values based on the specific type of boundary conditions, coupled with local characteristic decompositions. One-sided WENO approximations or reconstructions, which avoid using information from outside the computational domain, may also be used [135, 24].

The finite volume scheme (3.4), when discretized in time, can also be defined on a stag-

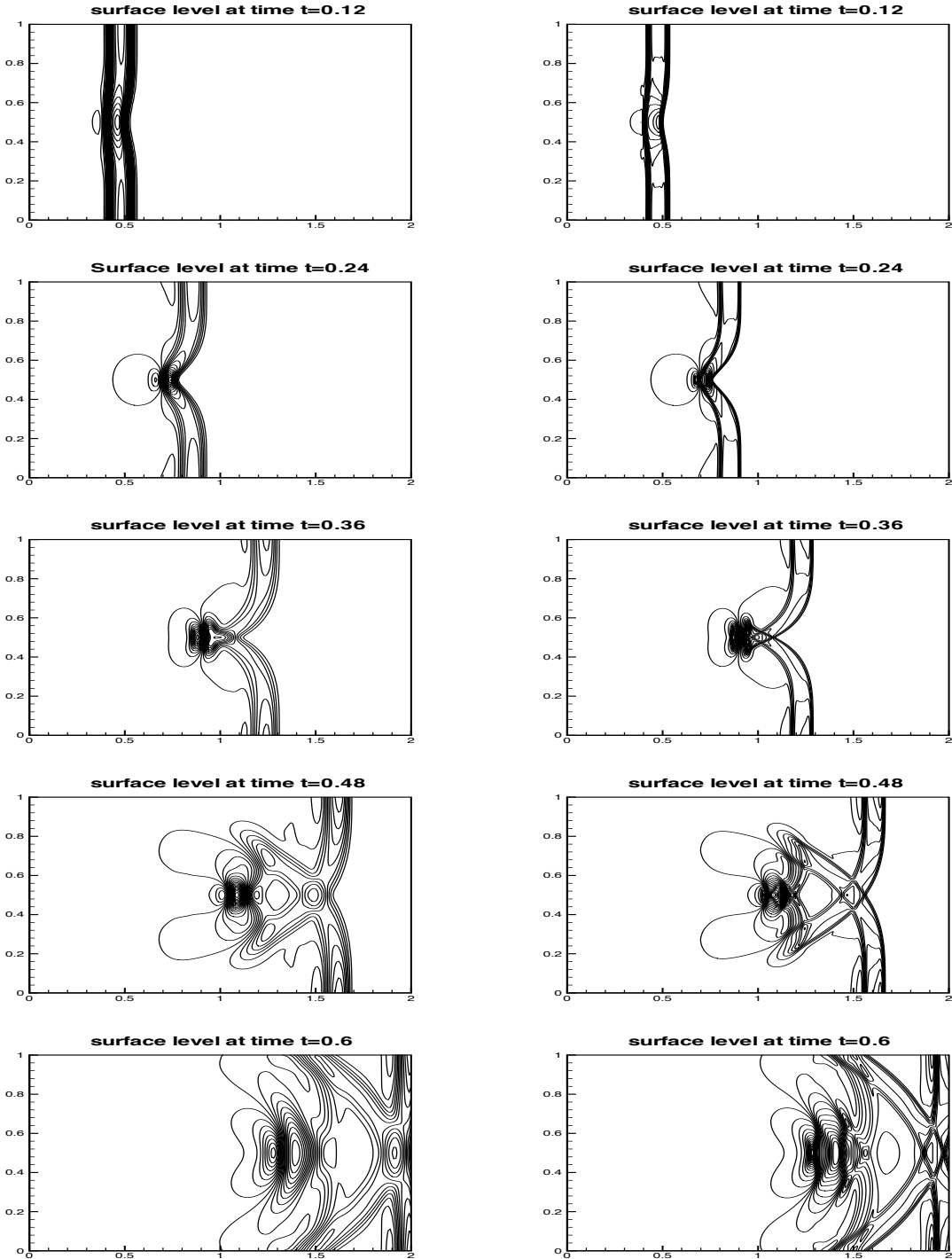


Figure 3.2: Two dimensional shallow water equation. Small (1%) perturbation from still water. Well balanced fifth order finite difference WENO scheme [161]. The contours of the water surface level. 30 uniformly spaced contour lines. From top to bottom: at time $t = 0.12$ from 0.999703 to 1.00629; at time $t = 0.24$ from 0.994836 to 1.01604; at time $t = 0.36$ from 0.988582 to 1.0117; at time $t = 0.48$ from 0.990344 to 1.00497; and at time $t = 0.6$ from 0.995065 to 1.0056. Left: results with a 200×100 uniform mesh. Right: results with a 600×300 uniform mesh.

gered mesh, resulting in a class of central schemes [109]. An advantage of such central schemes is that the numerical flux is computed in the smooth part of the reconstructed function, hence there is no need to use explicitly a monotone flux for the scalar case or a Riemann solver for the system case. WENO schemes based on the central scheme framework have been constructed in the literature, e.g. in [88, 89, 90, 124]. It seems that the central scheme framework allows the component-wise WENO reconstruction procedure to be used for less oscillatory results for third or even fourth order schemes, however for very high order central WENO schemes, characteristic WENO reconstruction is still necessary to obtain stable results [124]. A detailed assessment of component-wise versus characteristic reconstructions in the context of central WENO schemes is given in [124].

Finite volume WENO schemes on multi-dimensional structured meshes are straightforward to design [139]. Finite volume WENO schemes on two dimensional unstructured meshes are designed in [48, 71, 139, 42, 43]. For three dimensions, finite volume WENO schemes on unstructured meshes are designed in [42, 43, 184]. As we mentioned in Section 2.3, the WENO schemes in [48, 42, 43] choose the linear weights not to increase the order of accuracy of the approximation in each sub-stencil. Therefore these schemes do not achieve the optimal attainable order of accuracy for their stencil. However these schemes are easier to design since the linear weights can be chosen to be arbitrary positive constants, or to fit other constraints such as having larger linear weights for the more symmetric sub-stencils. The WENO schemes in [71, 139, 184] follow the traditional WENO procedure to obtain approximations on the larger stencil which are of higher order accuracy than that on each sub-stencil. Unfortunately, such schemes are very difficult to construct on unstructured meshes as the optimal linear weights depends on the local mesh distribution.

In [135], a multi-domain finite difference WENO scheme is designed. The computational domain can then be generalized to any region which can be covered by overlapping patches where for each patch a uniform Cartesian or a smooth curvilinear mesh suitable for a finite difference WENO scheme can be used. Information is transferred between patches via high

order interpolation. This multi-domain finite difference WENO scheme can be used in many practical situations, such as flow passing a wedge, with the cost of a finite difference scheme which is much smaller than that of a finite volume scheme. This scheme is used in [80] to study shock mitigation and drag reduction by pulsed energy lines.

Another attempt to expand the usability of the finite difference WENO method without increasing its cost is the design of residual distribution type finite difference WENO schemes for steady state conservation laws and convection dominated convection diffusion equations in [24, 25]. These schemes can be used on arbitrary *non-smooth* tensor product curvilinear meshes, are conservative, and have the same cost as the usual conservative finite difference schemes for two dimensional problems.

One difficulty of numerical solutions for conservation laws is that contact discontinuities, i.e. the discontinuities belonging to the characteristic field satisfying $\lambda'(u) \cdot r(u) \equiv 0$ where $\lambda(u)$ is an eigenvalue and $r(u)$ the corresponding eigenvector of the Jacobian $f'(u)$ of the conservation law (3.1), are much more difficult to resolve sharply than shocks. This is because the characteristics are parallel to the discontinuity for a contact discontinuity, while they converge into the discontinuity for a shock, see Figure 3.3. Therefore, a numerical shock is usually stable with a fixed number of transition points for long time simulation, while a numerical contact discontinuity may progressively become wider for longer time simulation. Strategies to improve the resolution of contact discontinuities for high order WENO schemes include the artificial compressibility method [169, 76], sub-cell resolution [62, 76], and the anti-diffusive flux correction method [40, 165]. We will use an example of shallow water with transport of pollutant [167] to demonstrate the performance of the anti-diffusive flux correction technique for high order WENO schemes developed in [165]. In Figure 3.4, we compare the performance of the regular fifth order WENO scheme and the anti-diffusive flux corrected fifth order WENO scheme for the resolution of pollutant. Comparing with the reference solution at the bottom of Figure 3.4, which is computed with the regular fifth order WENO scheme with an extremely refined mesh and can be considered as an exact

solution, the quality of the anti-diffusive WENO scheme is much better than that of the regular WENO scheme on the relatively coarse mesh with 300×100 points.

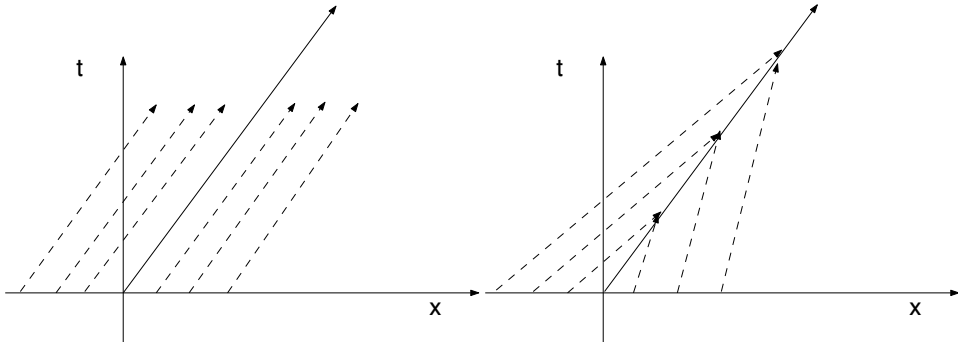


Figure 3.3: Characteristics. Left: contact discontinuity; right: shock.

For convection dominated convection diffusion equations, for example the Navier-Stokes equations with high Reynolds numbers, the WENO schemes discussed in previous subsections for conservation laws can be easily generalized. We can either use central difference approximations to the second derivative viscous terms of comparable order of accuracy, or absorb the evaluation of the viscous terms into the numerical fluxes by first computing an approximation to the first derivatives of the solution at cell interfaces to the desired order of accuracy. We refer to, e.g., [182, 185, 179, 180] for more details.

Since WENO schemes are explicit schemes, they can be implemented easily on massively parallel platforms. Large scale results obtained in, e.g. [45, 179, 180, 182, 185] are obtained by parallel WENO codes. The parallel efficiency of the high order WENO schemes is excellent.

4 WENO schemes for Hamilton-Jacobi equations

WENO schemes can be used also to solve PDEs which are not hyperbolic conservation laws. In this section we describe such an example. We consider WENO schemes for solving the following Hamilton-Jacobi equations

$$\varphi_t + H(\varphi_{x_1}, \dots, \varphi_{x_d}) = 0, \quad \varphi(x, 0) = \varphi^0(x), \quad (4.1)$$

where the Hamiltonian H is a (usually nonlinear) function which is at least Lipschitz continuous. H could also depend on φ , x and t in some applications, however the main difficulty for numerical solutions is the nonlinear dependency of H on the gradient of φ .

Hamilton-Jacobi equations appear often in many applications. One important application of Hamilton-Jacobi equations is the area of image processing and computer vision. Other application areas include, e.g. control and differential games.

The main difficulty in the numerical solutions of the Hamilton-Jacobi equation (4.1) is that global C^1 solution does not exist in the generic situation, regardless of the smoothness of the initial condition $\varphi^0(x)$. Singularities in the form of discontinuities in the derivatives of φ would appear at a finite time in most situations, thus the solutions would be Lipschitz continuous but no longer C^1 . In fact, at least in the one dimensional case, there is an equivalence between the Hamilton-Jacobi equation

$$\varphi_t + H(\varphi_x) = 0, \quad \varphi(x, 0) = \varphi^0(x) \quad (4.2)$$

and the hyperbolic conservation law

$$u_t + H(u)_x = 0, \quad u(x, 0) = u^0(x) \quad (4.3)$$

if we identify $u = \varphi_x$. As we have seen in Section 3, singularities for the conservation law (4.3) are in the form of discontinuities in the solution u , thus u is bounded, with a bounded total variation, but is not continuous. The results for the conservation law (4.3) can be directly translated to that for the Hamilton-Jacobi equation (4.2) by integrating u once. Discontinuities in u then become discontinuities for the derivative of φ .

For the one dimensional Hamilton-Jacobi equation (4.2), or for the multi-dimensional Hamilton-Jacobi equation (4.1) on a tensor product mesh, the WENO finite difference scheme [75] can be easily designed. We will use the one dimensional version (4.2) to demonstrate the idea. The WENO scheme in this case evolves the point values of the solution φ_i in the following way

$$\frac{d}{dt} \varphi_i + \hat{H}(u_i^-, u_i^+) = 0 \quad (4.4)$$

where $\hat{H}(u^-, u^+)$ is a monotone Hamiltonian, namely it is non-decreasing in its first argument u^- and non-increasing in its second argument u^+ , or symbolically $\hat{H}(\uparrow, \downarrow)$; it is consistent with the physical Hamiltonian $H(u)$, i.e. $\hat{H}(u, u) = H(u)$; and it is Lipschitz continuous with respect to both arguments u^- and u^+ . Monotone Hamiltonians can also be defined for multi-dimensional cases (4.1). We refer to, e.g. [114], for examples of monotone Hamiltonians in one- and multi-dimensional cases. The values u_i^\pm in (4.4) are WENO approximations to the derivatives of φ at the point x_i with a stencil one point biased to the left and one point biased to the right, respectively, described in Section 2.3. For example, a fifth order WENO scheme [75] uses the following stencil to approximate u_i^- :

$$S = \{x_{i-3}, x_{i-2}, x_{i-1}, x_i, x_{i+1}, x_{i+2}\}.$$

This stencil is the union of the following three sub-stencils

$$S_1 = \{x_{i-3}, x_{i-2}, x_{i-1}, x_i\}, \quad S_2 = \{x_{i-2}, x_{i-1}, x_i, x_{i+1}\}, \quad S_3 = \{x_{i-1}, x_i, x_{i+1}, x_{i+2}\}$$

The fifth order approximation u_i^- is, as usual, a convex combination of the three third order approximations to φ_x at $x = x_i$ based on the three sub-stencils S_1 , S_2 and S_3 respectively. Time discretization to the semi-discrete scheme (4.4) can again be based on the TVD Runge-Kutta time discretizations such as (3.5).

Unlike the case of conservation laws in Section 3, for the Hamilton-Jacobi equation (4.4) there is no finite volume scheme, and the finite difference scheme we described above does *not* have the restriction of uniform or smooth meshes. This finite difference scheme can be used on any mesh, smooth or not. For the multi-dimensional case (4.1), as long as we have a tensor product mesh, the finite difference WENO scheme can be trivially generalized, by simply computing approximations to the derivatives dimension by dimension. Thus the approximation to $u = \varphi_x$ is obtained by the one dimensional procedure described above along the x direction with y fixed, and the approximation to $v = \varphi_y$ is obtained by the same one dimensional procedure along the y direction with x fixed. WENO schemes can also be designed based on the central scheme framework, see, e.g. [8, 149]. However, a high order

WENO scheme to solve the multi-dimensional case (4.1) on unstructured meshes is much more involved. We refer to [183] for the details of high order WENO schemes solving two dimensional Hamilton-Jacobi equations on general triangulations; see also [87].

WENO schemes have been used widely in solving Hamilton-Jacobi equations from level sets [113]. For some of these application problems, for example for the problem of reinitialization of the signed distance function [152], one must solve steady state Hamilton-Jacobi equations repeatedly. One of the efficient methods to solve the steady state Hamilton-Jacobi equations is the so-called fast sweeping method. For high order WENO schemes, fast sweeping methods have been developed recently in [186].

Similar to the difficulty associated with the resolution of contact discontinuities in conservation laws, it is also difficult to resolve corners (discontinuities in the derivative of the solution) corresponding to a linearly degenerated Hamilton-Jacobi equation. In [166], the anti-diffusive flux correction technique in [165] for conservation laws is generalized to high order WENO schemes for solving Hamilton-Jacobi equations, to sharpen such corners. Numerical results in [166] demonstrate the good performance of this approach.

Finally, we mention that the convergence of a class of semi-Lagrangian large time step schemes, based on a WENO interpolation with the order of accuracy as high as 9, is proved in [13] for solving general viscosity solutions of convex Hamilton-Jacobi equations. This is the best theoretical convergence result obtained so far involving WENO schemes.

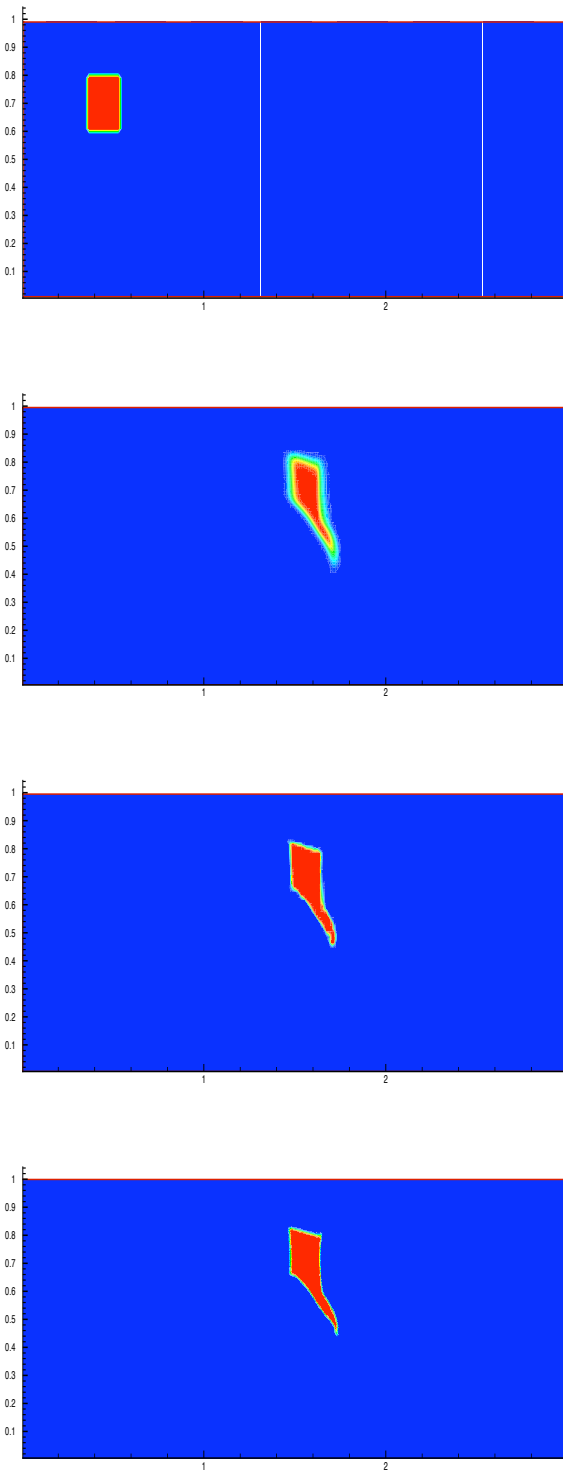


Figure 3.4: Shallow water equation coupled with the transport of pollutant. 300×100 uniform mesh. Contours of the pollutant T . Top: the initial pollutant. Second: pollutant obtained by the regular fifth order WENO. Third: pollutant obtained by the anti-diffusive fifth order WENO. Bottom: reference solution obtained by 1500×500 uniform mesh with regular fifth order WENO.

5 Relationship and comparison with other high order schemes

In this section we would like to briefly describe a few competitive types of numerical methods for solving convection dominated problems. Rather than surveying the details of these methods, we emphasize efforts in combining the advantages of these methods and the WENO procedure. Comparisons of some of these schemes with WENO schemes can be found in [187, 144].

5.1 Discontinuous Galerkin method

Discontinuous Galerkin methods are a class of finite element methods that have gained a lot of popularity in recent years, e.g. [31, 32, 37]. For our purpose, the discontinuous Galerkin methods can also be viewed as a generalized finite volume method for solving conservation laws. For the one dimensional conservation law (3.1), instead of integrating it in the cell $I_i = (x_{i-\frac{1}{2}}, x_{i+\frac{1}{2}})$ to obtain the integral form (3.3), which forms the basis of the finite volume scheme (3.4), we multiply the PDE (3.1) by a test function v and then integrate it in the cell I_i to obtain, after an integration by parts

$$\int_{x_{i-\frac{1}{2}}}^{x_{i+\frac{1}{2}}} u_t v dx - \int_{x_{i-\frac{1}{2}}}^{x_{i+\frac{1}{2}}} f(u) v_x dx + f(u_{i+\frac{1}{2}}) v_{i+\frac{1}{2}} - f(u_{i-\frac{1}{2}}) v_{i-\frac{1}{2}} = 0 \quad (5.1)$$

To convert (5.1), which is satisfied by the exact solution u of the PDE (3.1) and any test function v , to a discontinuous Galerkin scheme, we would like to replace u and v by functions in a finite dimensional piecewise polynomial space $V_{\Delta x}$ defined by

$$V_{\Delta x} = \{v : v|_{I_j} \in P^k(I_j), j = 1, \dots, N\}$$

with $P^k(I_j)$ denoting the set of polynomials of degree up to k defined on the cell I_j . However, the boundary terms $u_{i+\frac{1}{2}}$ and $v_{i+\frac{1}{2}}$ etc. would not be well defined for functions in $V_{\Delta x}$, since they are discontinuous exactly at such cell interfaces. If we take $v = 1_{I_i}$ to be the indicator function of cell I_i , that is, $v(x) = 1$ when $x \in I_i$ and $v(x) = 0$ otherwise, then (5.1) becomes

the integral form (3.3) which forms the basis of the finite volume scheme (3.4). We hope that the discontinuous Galerkin scheme would be of the same form as the finite volume scheme (3.4) for this choice of v , which motivates the choice of the interface values as follows:

1. $f(u_{i+\frac{1}{2}})$ is replaced by a single valued monotone numerical flux $\hat{f}_{i+\frac{1}{2}} = \hat{f}(u_{i+\frac{1}{2}}^-, u_{i+\frac{1}{2}}^+)$ which depends on both the left and right values of u at the cell interface $x_{i+\frac{1}{2}}$. Naturally, $f(u_{i-\frac{1}{2}})$ is replaced by $\hat{f}(u_{i-\frac{1}{2}}^-, u_{i-\frac{1}{2}}^+)$.
2. The test function v is replaced by its values inside the relevant cell, that is, by $v_{i+\frac{1}{2}}^-$ at the right boundary of cell I_i and by $v_{i-\frac{1}{2}}^+$ at the left boundary of cell I_i .

Thus the discontinuous Galerkin scheme is: find $u \in V_{\Delta x}$ such that

$$\int_{x_{i-\frac{1}{2}}}^{x_{i+\frac{1}{2}}} u_t v dx - \int_{x_{i-\frac{1}{2}}}^{x_{i+\frac{1}{2}}} f(u) v_x dx + \hat{f}_{i+\frac{1}{2}} v_{i+\frac{1}{2}}^- - \hat{f}_{i-\frac{1}{2}} v_{i-\frac{1}{2}}^+ = 0 \quad (5.2)$$

for all $v \in V_{\Delta x}$.

Notice that by taking the test function $v = 1_{I_i} \in V_{\Delta x}$ we obtain the same identity as the finite volume scheme (3.4). Therefore we may claim that the discontinuous Galerkin scheme (5.2) is a generalized finite volume scheme. However, an essential difference between the finite volume scheme (3.4) and the discontinuous Galerkin scheme (5.2) is that the finite volume scheme evolves only one piece of information per cell, namely the cell average \bar{u}_i . If higher order point values $u_{i+\frac{1}{2}}^\pm$ are needed at the cell interfaces, they will be reconstructed by the WENO procedure. On the other hand, the discontinuous Galerkin scheme evolves the whole polynomial per cell I_i (if the polynomial is of degree k then $k+1$ pieces of information is evolved per cell). This increases the storage and computational cost for the evolution, however it then eliminates the cost of reconstruction completely.

Since the WENO procedure is only applied at the reconstruction stage of the finite volume scheme, it cannot be directly used within the framework of a discontinuous Galerkin scheme. Therefore, discontinuous Galerkin schemes rely on limiters to control spurious oscillations. See, e.g. [28, 27, 30].

The discontinuous Galerkin methods are more flexible than the finite volume WENO schemes for solving conservation laws on multi-dimensional unstructured meshes. This is because the discontinuous Galerkin methods do not involve the reconstruction procedure, which tends to be very complicated for unstructured meshes. However, the discontinuous Galerkin methods are less robust in dealing with solutions with strong shocks. This is because the state of the art for limiters is less advanced than the WENO procedure in controlling spurious oscillations without affecting accuracy for smooth structures.

Recently, efforts have been made in the following two directions to combine the advantages of WENO and discontinuous Galerkin schemes:

1. The design of Hermite type WENO schemes. These are schemes between the finite volume WENO scheme, which evolves only one piece of information per cell, and the discontinuous Galerkin scheme, which evolves $k + 1$ pieces of information per cell for a $(k + 1)$ -th order method in one dimension using piecewise polynomials of degree k . The Hermite WENO schemes designed in [126, 129, 130] evolve a linear function per cell (hence they evolve 2 pieces of information per cell in one dimension) and reconstruct the necessary point values to higher order accuracy when necessary. Because each cell contains more than one degrees of freedom, the reconstruction would involve a narrower stencil for the same order of accuracy, resulting in more compact WENO schemes.
2. The design of WENO limiters for the discontinuous Galerkin schemes. The idea is to first identify the so-called “troubled cells”, then retain only the cell average information in such cells for the purpose of conservation, and use the WENO procedure to reconstruct the higher order moments of the polynomials in such cells using the information from neighboring cells. Both the traditional WENO reconstruction technique and the Hermite WENO reconstruction technique (which is more desirable since it involves a narrower stencil) can be used. This approach has been pursued in [127, 126, 129]. The issue of effective “troubled cell” indicators has been addressed in [128].

5.2 Compact schemes

Compact schemes are finite difference schemes where the derivatives are approximated not by polynomial operators but by rational function operators on the discrete solutions. For example, a fourth order central compact approximation to the first derivative is given by

$$\frac{1}{6} ((u_x)_{i-1} + 4(u_x)_i + (u_x)_{i+1}) = \frac{1}{2\Delta x} (u_{i+1} - u_{i-1}) \quad (5.3)$$

Clearly, a tridiagonal linear solver is needed to obtain the approximation $(u_x)_i$ for all i from (5.3). From this point of view, compact approximations to derivatives are not really compact, since the approximation to $(u_x)_i$ involves contributions from all the grid values u_j . We refer to, e.g. [70, 85] for the general discussion of compact schemes. Upwind (rather than central) compact schemes are developed in [29].

The main advantage of compact schemes is that they have better resolution power for high frequency waves than the usual finite difference schemes of the same order of accuracy. Therefore, they are especially suitable for problems involving long time evolution of waves, such as turbulence simulations [85].

Efforts have been made in the literature to develop hybrid compact WENO schemes. In [79], a compact WENO scheme is designed where the WENO procedure is used on the explicit part of the scheme (the right hand side of (5.3)). In [115], a hybrid compact-WENO scheme is developed to solve shock turbulence interaction problems. A shock detector is used to find regions where the WENO approximation is used instead of the usual compact difference approximation. In [39], the WENO procedure is used to build nonlinear WENO compact schemes.

5.3 Spectral method

For smooth problems in regular geometry, the spectral method [51, 12] is the most powerful method to obtain accurate results, especially for long time wave propagation problems. Fourier or Chebyshev spectral methods are also very efficient because of the Fast Fourier

Transforms. However, it is a challenge to design stable spectral schemes for solving convection dominated problems which have sharp gradient regions or shocks. Even though spectral methods with a carefully designed application of filters can produce very good results for shock wave calculations [41], such methods are not robust, in the sense that the application of filters requires experience in order to maintain stability without destroying accuracy.

Efforts have been made in the literature to develop hybrid spectral WENO schemes. In [35, 34], a hybrid spectral WENO method, using the WENO procedure near strong shocks and spectral procedure elsewhere, is developed and demonstrated to give good numerical results for a few quite demanding test problems.

5.4 Wavelets and multi-resolution methods

Wavelets and multi-resolution methods are powerful frameworks to solve multi-scale problems containing a wide range of physical scales. In applications to solve convection dominated PDEs, the multi-resolution framework of Harten [63] is particularly attractive, since it utilizes the essential ideas of wavelets in their effective multi-resolution decomposition in combination with features in conservative schemes for hyperbolic conservation laws relying on high order reconstruction. There have been numerous works since then combining Harten's multi-resolution framework with high order, high resolution schemes, see for example [7, 23]. Recently, this multi-resolution framework has also been combined with the WENO procedure in [9] to produce an adaptive multiresolution WENO scheme for solving conservation laws.

5.5 Dispersion optimized finite difference schemes

For application problems in which waves must propagate over a long time with a relatively coarse mesh (that is, the number of grid points per wave is not large), such as problems in aeroacoustics and electro-magnetism, it is important to maintain the phase accuracy of the waves to the best extent possible. Spectral methods are the best choice to maintain such phase accuracy. Compact schemes discussed in Section 5.2 are also good choices. If one must

use explicit finite difference schemes, then there is a systematic approach [153] to modify the coefficients of the finite difference approximation, with the objective of increasing the phase resolution (dispersion relation) at the price of lowering the order of accuracy for the same stencil. Even though such dispersion optimized finite difference schemes are less accurate for asymptotically small mesh sizes (that is, when the number of points per wave is large), they are better than the usual finite difference schemes on the same stencil for marginally resolved waves (that is, when the number of points per wave is small).

Even though WENO schemes are nonlinear, they can also be adapted by such dispersion optimized technique to enhance their resolution power for marginally resolved waves. Efforts are made in the literature [98, 119, 159, 105] to design such dispersion optimized WENO schemes and to apply them for turbulence simulations.

6 Applications

The WENO schemes discussed in previous sections have been used in many physical and engineering applications. In this section we briefly summarize some of these applications with the objective of giving a glimpse of the diversity of possible applications of the WENO methodology, rather than providing an exhausting list. Most of these applications have a common feature: they are solving for solutions with both discontinuities or sharp gradient regions and complicated smooth region structures.

6.1 Computational fluid dynamics

The largest application area of WENO schemes is the area of computational fluid dynamics (CFD). Besides the applications already mentioned in previous sections, we mention as additional examples the following representative works.

1. Shock vortex interaction is an important physical process for sound generation, and it is a simple model for shock turbulence interaction. This problem has complicated solutions where shocks of various strengths and vorticity flows co-exist, which makes it

ideal to be simulated by high order WENO schemes. Many papers in the literature use WENO scheme to study the details of shock vortex interactions in different physical setup and regimes, for example [57, 116, 117, 131, 179, 180]. See also related work in blast wave/vortex interaction and sound generation in [21]; shock wave-thermal inhomogeneity interactions in [58]; reflected shock/vortex interaction near an open-ended duct in [93]; and shock/vortex interactions induced by blast waves in [94]. As an example of shock vortex interaction, in Figure 6.1 we plot the shadowgraphs (contours of $\nabla^2 \rho$ where ρ is the density) of an oblique Mach 1.2 shock with a strong colliding vortex pair simulated by the fifth order WENO scheme for the compressible Navier-Stokes equations [180]. We can see clearly that complicated flow structure from the shock vortex interaction is resolved well by the fifth order WENO scheme.

2. High speed and turbulent flows typically contain both strong shocks and complicated flow structures, making WENO schemes good simulation tools for them. Supersonic jet and shear layers are studied in [22]. Turbulent flows in high-speed aerodynamics are studied in [60]. Turbulence spectra characteristics for direct and large eddy simulations are studied in [82]. Hypersonic aerodynamic heating prediction is made in [84]. The starting process in a supersonic nozzle is studied in [108]. Direct numerical simulation and analysis of a spatially evolving supersonic turbulent boundary layer at $M=2.25$ are performed in [118]. Instability wave generation and propagation in supersonic boundary layers are studied in [78]. Large eddy simulation of the shock wave and boundary layer interaction is performed using the hybrid compact/WENO scheme in [154]. Implicit WENO schemes for the compressible and incompressible Navier-Stokes equations are developed in [170, 171] and used to perform the three-dimensional wing flow computations in [172]. Computation of supersonic turbulent flowfield with transverse injection is performed in [151]. The stochastic piston problem is studied in [97]. Nearly-incompressible, inviscid Taylor-Green vortex flow is studied in [145].

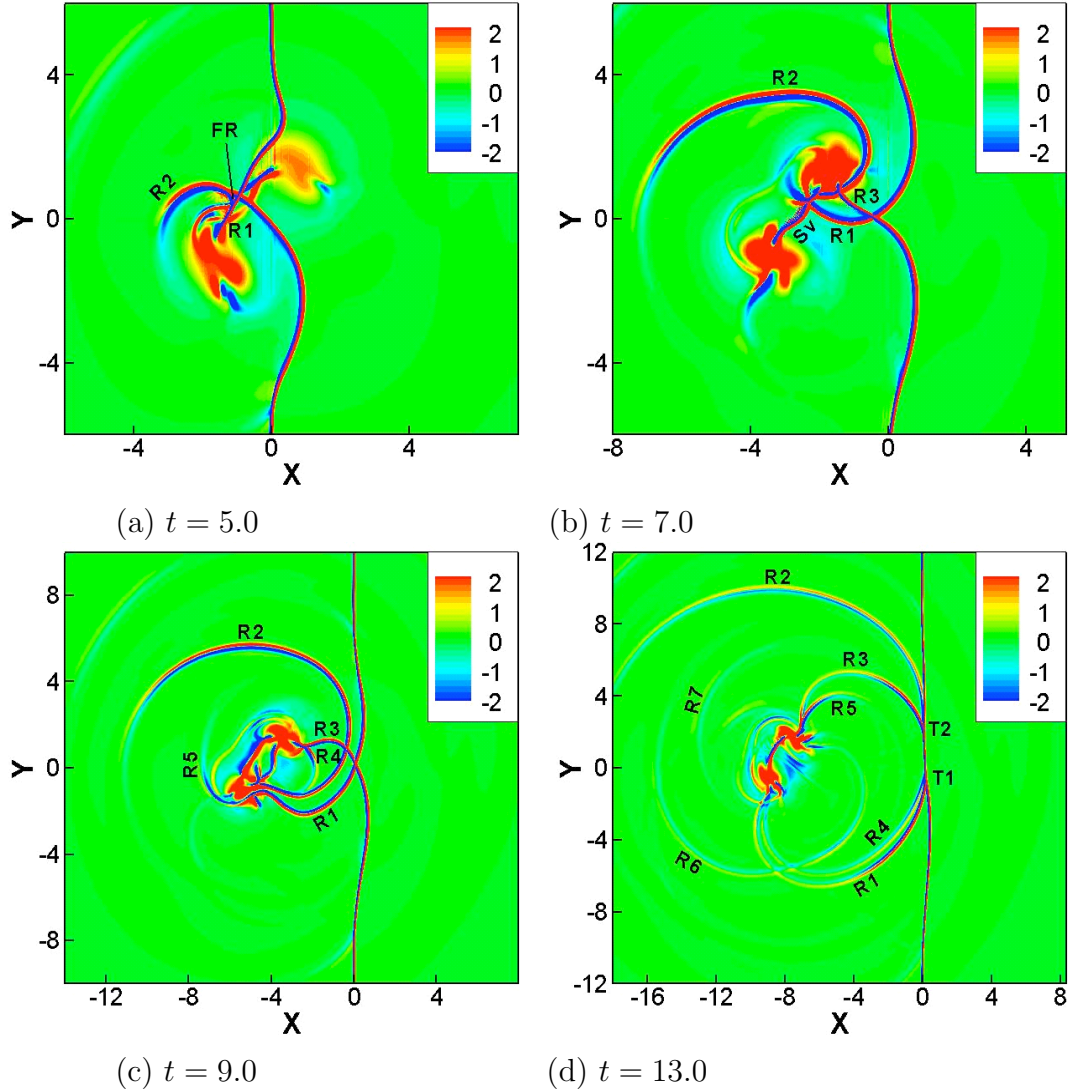


Figure 6.1: Fifth order WENO simulation of the evolution of an oblique shock and a colliding vortex pair interaction [180]. Shock Mach number $M_s = 1.2$, vortex Mach number $M_\nu = 0.8$, and angle of the oblique shock wave $\alpha = 45^\circ$.

3. Reacting flows, detonations, and flames contain multiple scales in the solution together with shocks, making the numerical simulation of them very difficult. WENO schemes have been successfully used for such simulations. Reacting flows with complicated solution structure are studied in [2]. Pulse detonation engine phenomena are studied in [67]. A very accurate simulation of pulsating one-dimensional detonations is performed in [68, 69]. The structure and evolution of a two-dimensional H-2/O-2/Ar cellular detonation are studied in [72]. A unified model for the prediction of laminar flame transfer functions is built, and comparisons are made between conical and V-flame dynamics in [134]. Modeling tools for the prediction of premixed flame transfer functions are studied in [133].
4. An interesting application of shock mitigation and drag reduction by pulsed energy lines for supersonic flows past a wedge is studied in [80] using the multi-domain finite difference WENO scheme developed in [135]. The simulation results indicate a saving of energy (energy gained is larger than energy spent to generate the pulsed energy lines) for all studied configurations.
5. A WENO finite difference scheme for solving the magnetohydrodynamics (MHD) flows is developed in [77]. This code is used in, e.g. [160] to study the dynamical evolution of coherent structures in intermittent two-dimensional MHD turbulence.
6. Real gas computation using an energy relaxation method is performed in [107]. Compressible multicomponent flows are simulated in [102, 104]. A pseudocompressibility method for the numerical simulation of incompressible multifluid flows is developed in [112]. Modeling and simulation for a particle-fluid two phase flow problem are studied in [177].
7. Hydrodynamic and quasi-neutral approximations for collisionless two-species plasmas are performed in [81]. Effects of shock waves on Rayleigh-Taylor instability are studied in [185]. An example of the Rayleigh-Taylor instability with or without shock waves is

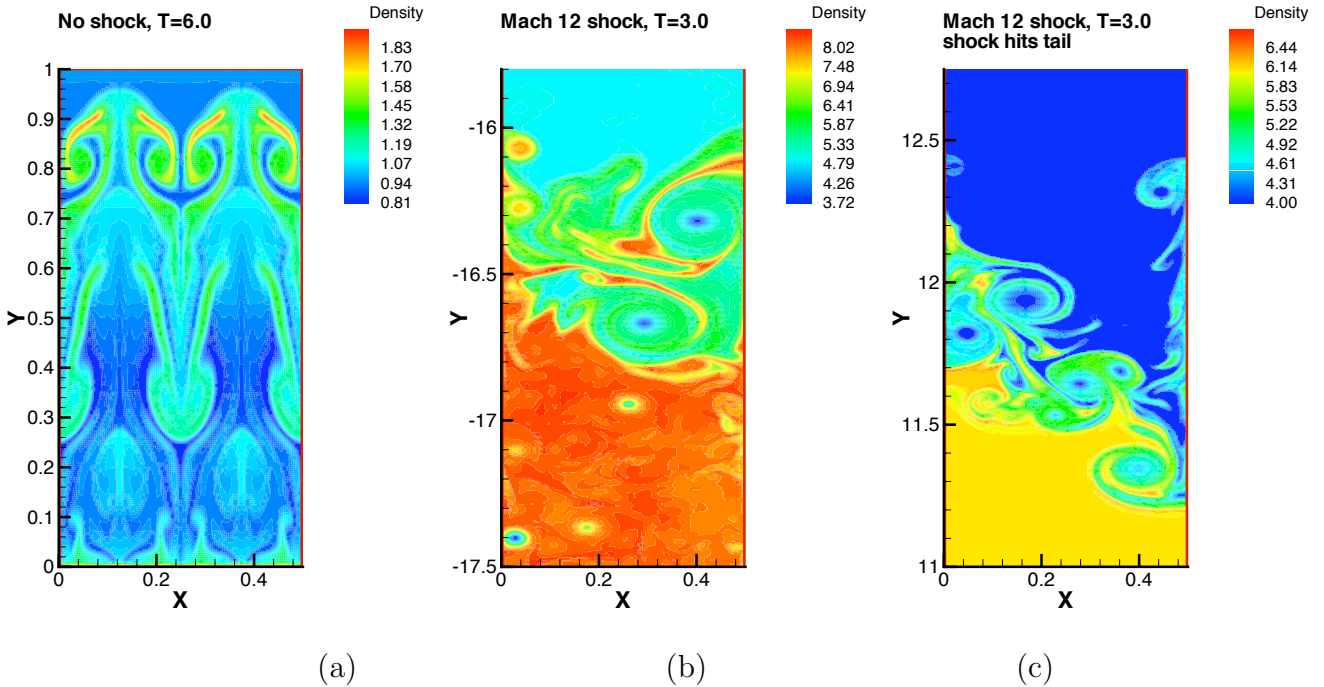


Figure 6.2: Ninth order WENO simulation of the Rayleigh-Taylor instability with or without shock waves [185]. Left (a): the Rayleigh-Taylor flow at $T = 6.0$; middle (b): Mach 12 shock hitting the Rayleigh-Taylor interface from the top, $T = 3.0$; right (c): Mach 12 shock hitting the Rayleigh-Taylor interface from the bottom, $T = 3.0$. Density ρ .

shown in Figure 6.2, in which a Rayleigh-Taylor flow (left picture) is compared with the flow of a Mach 12 shock hitting the Rayleigh-Taylor interface from the top (middle picture) and from the bottom (right picture) [185]. The simulation is performed by a ninth order WENO scheme, which seems to resolve the complicated flow structures in the presence of strong shocks very well. We can clearly observe that the shock waves do speed up the transition of the Rayleigh-Taylor flow to full instability in each case.

8. Shallow water equations and sediment transport equations are studied in [36]. Two-dimensional shallow water equations are simulated by composite schemes (for which WENO is a component) in [100], see also [99]. Underwater blast-wave focusing is studied in [92]. Non-breaking and breaking solitary wave run-up is studied in [91]. See also [158, 161, 163, 164] for well balanced high order WENO schemes for the shallow water equations.

9. Numerical simulation of interphase mass transfer with the level set approach is performed in [168]. Migrating and dissolving liquid drops are studied in [5, 6]. For flows in liquid helium, nonlinear effects and shock formation in the focusing of a spherical acoustic wave are studied in [3].
10. A WENO scheme is designed in [16] for the Lifshitz-Slyozov system, which models the formation of a new phase in solid mechanics. This is not exactly fluid mechanics but the type of PDEs and difficulties in their numerical solutions are similar.
11. Several different discretization techniques are studied and compared in [95] for the transport and diffusion equations in chemical engineering problems. WENO schemes are found to be efficient and essential for numerical schemes which use relatively small number of mesh points. In [96], WENO schemes are applied to solve the population balance equations in chemical engineering and are found to be accurate and economical for this application.
12. A careful numerical study is performed in [140] for Euler equations and in [182] for Navier-Stokes equations to demonstrate that for flow problems containing both shocks and complicated smooth region structures, it is more economical to use high order WENO schemes than to use lower order schemes to achieve the same level of resolution. See also [174] for a comparison of schemes (including the WENO scheme) for the resolution of contact discontinuity layers, in which the WENO schemes performed nicely.

6.2 Astronomy and astrophysics

Applications in astronomy and astrophysics are closely related to that in fluid dynamics described in the previous subsection. This is because many models in astronomy and astrophysics (hydrodynamic, radiative transfer, etc.) are very similar to those in fluid dynamics. We mention in particular the following applications in which WENO schemes were success-

fully used.

1. A hybrid cosmological WENO hydrodynamic/N-body code is developed in [45] and applied to study many astrophysical phenomena in, e.g. [44, 74, 66]. In particular, the high resolution power and small numerical viscosity of the WENO code allow the authors to study the turbulence-like behavior for the low-redshift cosmic baryon fluid on large scales in [66]. A relativistic adaptive mesh refinement WENO hydrodynamics code (RAM) is developed in [181].
2. Dynamical response of a stellar atmosphere to pressure perturbations is studied in [38].
3. The radiative transfer and ionized sphere at reionization are studied in [123, 121].
4. The boundary layer between a white dwarf and its accretion disk is studied by a numerical code based on WENO ideas in [47].
5. Numerical simulation of high Mach number astrophysical jets with radiative cooling is performed in [59]. Because of the very high Mach number shock (Mach=80) involved in the simulation, many high resolution schemes become unstable but the WENO code is able to resolve the solution well.

6.3 Semiconductor device simulation

WENO schemes have been used to solve various models in semiconductor device simulations. The earlier studies were mostly for moment models such as the hydrodynamic and energy transport models, however more recent study has been focused on solving kinetic type models such as the BGK-Poisson models and Boltzmann-Poisson models. We mention in particular the following representative works. WENO schemes are again showing their robustness in such simulations, especially when the grid is very coarse (due to the computer storage and speed limitation because of the high dimensions in the models) and hence the solution variation between neighboring grids is large in certain regions. Traditional schemes often

fail or perform poorly for such coarse meshes even though they are stable for more refined meshes. The advantage of the WENO schemes is thus in its stability and resolution power on such coarse meshes.

1. A WENO solver is designed for solving the Boltzmann-Poisson system in semiconductor device simulations in [14, 15]. In its most general context, this system involves a transport equation with collision source terms in three space dimensions, three phase velocity dimensions, plus time (6+1 dimensions), coupled with a Poisson equation in three space dimensions. A direct simulation to this full system is still very difficult, if not impossible, even on today's most powerful parallel computers. A dominate simulation tool for such systems is the direct simulation Monte-Carlo (DSMC) method. Even though DSMC is relatively easy to code and to use, it produces noisy results and also is difficult to generate probability density functions (pdf's), especially in a time dependent dynamic setting. Because of the good resolution power and nonlinear stability of the WENO algorithm, the WENO solver can be applied to devices with two space dimensions and three phase velocity dimensions, plus time, using a coarse mesh on a single PC, obtaining results which compare well with DSMC results. The advantage of this WENO solver over the traditional Monte-Carlo simulations include the noise-free resolution and the ability to produce the probability density functions in the dynamic regime. It is argued in [11] that the WENO solver can be an effective tool to help improve the Monte-Carlo simulators, in such aspects as the charge assignment to the mesh, the treatment of the boundary conditions and the free flight duration, where well accepted rules do not exist for DSMC. See also related work in [49]. We present in Figure 6.3 an example of the pdf's at various physical locations of a two dimensional MOSFET device (a 5-dimensional plus time simulation) by a fifth order WENO code on a relatively coarse mesh with 49×33 points in space and $66 \times 12 \times 12$ points in the velocity space [15]. The code runs on a standard PC and reaches steady states in 3 days. We can clearly see that the pdf profiles have rapidly changing layers

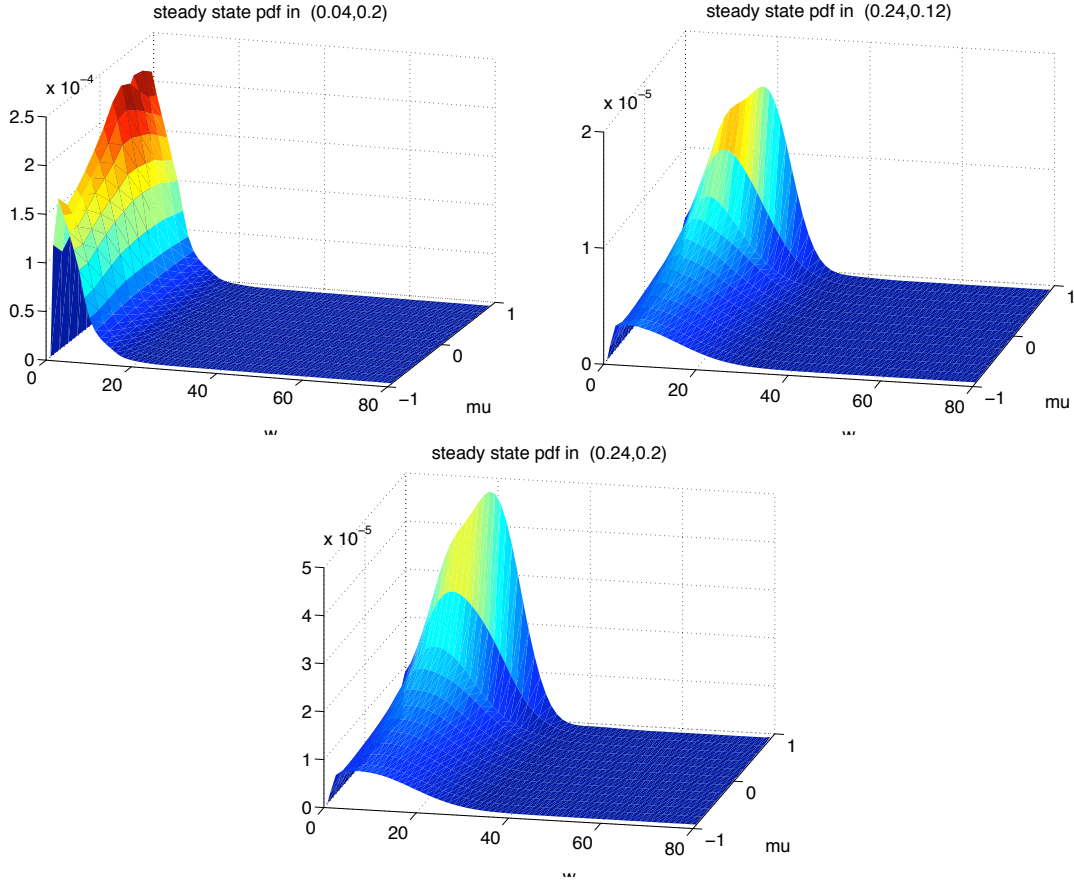


Figure 6.3: MOSFET device. Boltzmann-Poisson system. Fifth order WENO code on a coarse $49 \times 33 \times 66 \times 12 \times 12$ mesh [15]. Pdf's in steady state averaged over ϕ at different locations of the MOSFET. Top left: at $(x, y) = (0.04, 0.2)$; top right: at $(x, y) = (0.24, 0.12)$; bottom: at $(x, y) = (0.24, 0.2)$.

for such coarse meshes, and the WENO code produces stable results which are quite accurate, when compared with simulation results with more refined meshes obtained on a parallel computer.

2. WENO scheme is used in [19] for the simulation and comparison of kinetic (BGK relaxation model), hydrodynamic, and high-field models for semiconductor devices. It is also used to numerically verify the Child-Langmuir limit for semiconductor devices in [10].

6.4 Traffic flows

Traffic flows are often modelled by hyperbolic type partial differential equations. WENO schemes have been successfully used in the following traffic flow applications.

1. A finite difference WENO scheme is designed for a multi-class Lighthill-Whitham-Richards traffic flow model in [175]. An extension of the multi-class traffic flow model to an inhomogeneous highway, involving the physical location x -dependent fluxes which may be discontinuous in x , is studied in [176].

The traffic flow model in [175] is a large system of hyperbolic conservation laws. The number of equations in this system is the number of different classes of drivers, which is taken to be as large as 9 in the simulation in [175]. For this system, it is difficult to explicitly construct the exact Riemann solver. One would then typically use an approximate Riemann solver such as the Lax-Friedrichs solver. In the top left picture in Figure 6.4, we plot the numerical solution of traffic density of the first order Lax-Friedrichs scheme with 6400 grid points and of the fifth order WENO scheme with 100 grid points. If we only use the first order Lax-Friedrichs scheme in the simulation, we might be satisfied with a grid refinement study using 400, 800, 1600, 3200 and 6400 grid points, since 6400 points sound plenty. However, the numerically converged solution for this problem contains 9 small staircases and can be seen in the top right picture in Figure 6.4 (the one with 1600 grid points of the fifth order WENO scheme, which basically agrees with the result using 400 grid points of the fifth order WENO scheme). From the bottom left picture in Figure 6.4, we can see that the first order Lax-Friedrichs scheme also slowly converges to the staircase solution, but it needs as many as 25600 grid points to achieve a resolution comparable to the fifth order WENO scheme with 400 grid points. This is a very good example to demonstrate the power of high order schemes: if one uses only the first order scheme, one might miss important solution features (the stairs) completely since one might stop the simulation

prematurely with a 6400 point grid, which would seem to be refined enough. Also, from a computational efficiency point of view, it is much more economical to use the fifth order WENO scheme with 400 points to achieve the same resolution as the first order scheme with 25600 points.

2. A reactive dynamic user equilibrium model for pedestrian flow using a continuum modeling approach is constructed in [73]. A two-dimensional walking facility that is represented as a continuum within which pedestrians can freely move in any direction is considered. A pedestrian chooses a route to minimize the travel cost to the destination in a reactive manner, based on the instantaneous information. The pedestrian demand is time varying. The pedestrian density, flow flux, and walking speed are governed by the conservation equation. A general speed-flow-density relationship is considered. The problem is formulated by the flow conservation equation, which is a time dependent conservation law, coupled with a static Hamilton-Jacobi equation at each fixed time t . An efficient and stable discretization for these coupled PDEs is designed in [73] using the high order WENO schemes for both the flow conservation law and the static Hamilton-Jacobi equation. Accelerating techniques such as the fast sweeping method for solving the static Hamilton-Jacobi equation have been used.

6.5 Computational biology

Many problems in computational biology involve models which are hyperbolic or otherwise convection dominate. We mention the following applications where WENO schemes were developed and used.

1. A high order, well-balanced WENO finite difference scheme is designed in [46] to study a hyperbolic model describing chemosensitive movement, in which cells change their direction reacting to the presence of a chemical substance, approaching chemically favorable environments and avoiding unfavorable ones. Such chemosensitive movement includes chemokinesis, which describes non-directed bias in the movement behavior in-

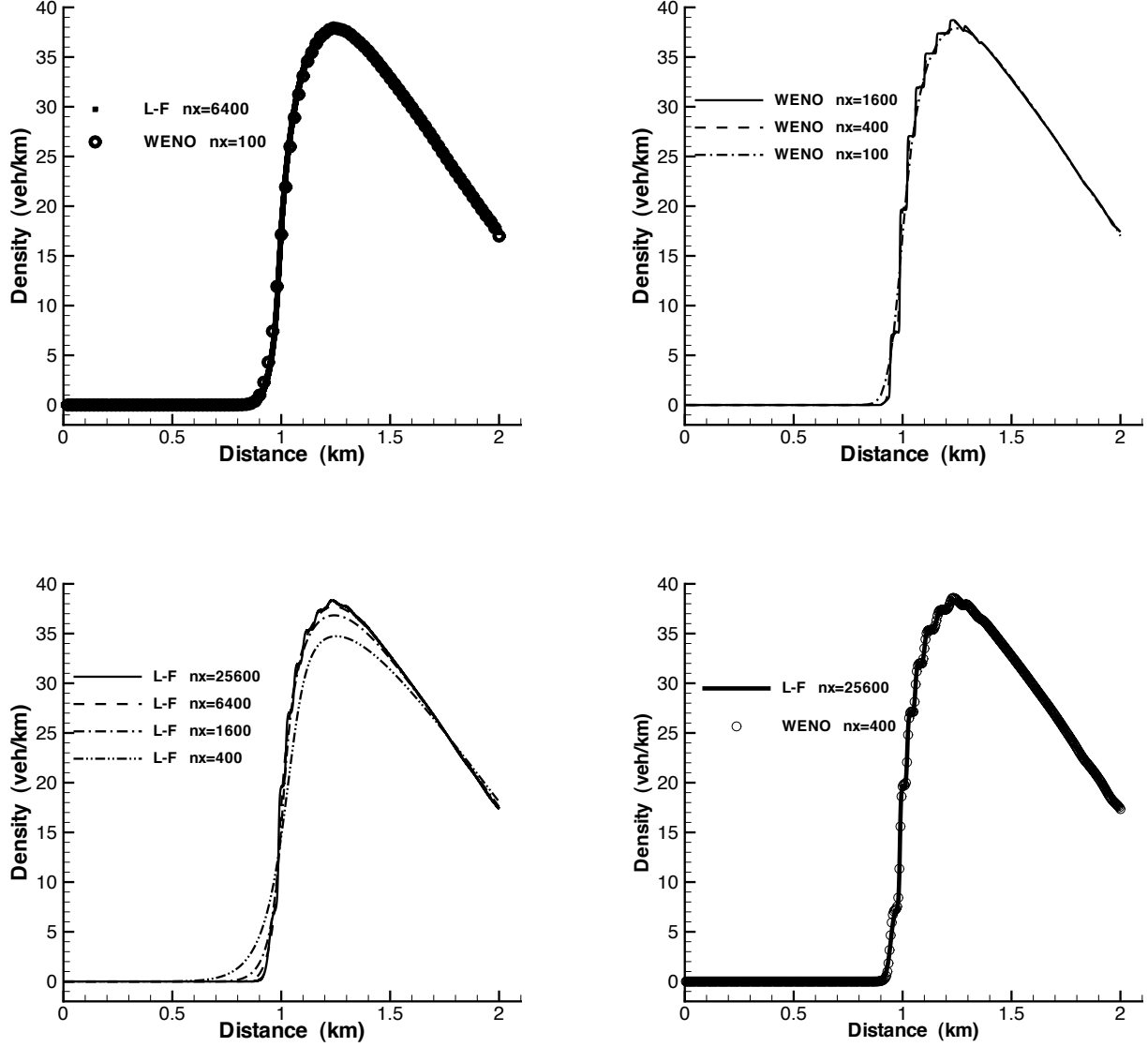


Figure 6.4: 9-class traffic flow model [175]. Density versus distance. Top left: Comparison between the first order Lax-Friedrichs scheme with 6400 points (solid line) and the fifth order WENO scheme with 100 points (circles). Top right: Convergence of the fifth order WENO scheme with 100 points (dash-dot line), 400 points (dashed line) and 1600 points (solid line). Bottom left: Convergence of the first order Lax-Friedrichs scheme with 400 points (dash-double dots line), 1600 points (dash-dot line), 6400 points (dashed line) and 25600 points (solid line). Bottom right: Comparison between the first order Lax-Friedrichs scheme with 25600 points (solid line) and the fifth order WENO scheme with 400 points (circles).

directly leading to an oriented movement of the population, and chemotaxis, which denotes a directed orientation towards or away from a chemical stimulus. The high order WENO method gave much better resolution than lower order methods in demonstrating formation of networks in the hyperbolic models similar to those observed in experiments.

2. A hydrodynamic model to describe an open ionic channel flow is developed in [20]. This model is a hyperbolic conservation law system with heat conduction terms and source relaxation terms coupled with a Poisson equation. An high order ENO solver was used in [20], and followup work was performed by using a WENO solver. The high order ENO/WENO solver provided an efficient tool to study the details of ionic channel flows.
3. A high order WENO scheme is designed for a hierarchical size-structured population model with nonlinear growth, mortality and reproduction rates in [138], following up on the work in [137] in which stability and convergence are proved for a second order TVD type high resolution scheme. The hierarchical structured population model describes population dynamics in which the size of an individual determines its access to resources and hence to its growth or decay. This dependency is based on the environment which is a global function of the density for all sizes. Therefore, a special feature of this model is that the boundary condition at the size $x = 0$ involves a function g representing the growth rate of an individual which is global in the size space. There is also a global size dependency of the coefficients in the conservation law. This makes it difficult to design stable and accurate numerical schemes. As for traditional conservation laws, the solutions to this hierarchical size-structured population model also contain discontinuities. The high order WENO scheme developed in [138] can obtain much more accurate results than the second order scheme in [137] for the same meshes.

7 Concluding remarks

We have given a review on the algorithm design, analysis, implementation and application of high order WENO schemes for solving convection dominated problems. The extensive list of applications mentioned in this paper, or contained in the references and their references therein, would hopefully convince the readers the wide applicability of WENO schemes. We mention in this last section a few topics which are currently being investigated about WENO schemes:

1. Efficient and robust implicit time discretization involving WENO spatial discretizations. This would be helpful for situations with significant diffusion in some regions for a convection-diffusion equation, or in an adaptive environment where the grid size might be very small in some regions. It would also be useful for computing steady state solutions. The difficulty here is the high level of nonlinearity in the nonlinear weights. For a fully implicit discretization, the resulting nonlinear system at each iteration is costly to solve, and certain iterative procedures such as the Newton's method does not seem to be robust near strong shocks for a large time step [53]. Preliminary study has been made to investigate the possibility of freezing some of the nonlinear weights in the time discretization [55]. More study is needed to obtain a robust and efficient approach for multi-dimensional systems containing strong shocks.
2. Different designs of nonlinear weights for specific purposes. Examples of such designs include the modified nonlinear weights to enhance accuracy in smooth regions, especially at smooth extrema [68], discussed in Section 2.3; the modified weights to improve steady state convergence [178], discussed in Section 2.3; and the dispersion optimized WENO schemes [98, 119, 159, 105], discussed in Section 5.5. It can be imagined that different design of the nonlinear weights tailored towards specific class of problems would enhance the accuracy, stability and other good properties of the WENO scheme.

3. While WENO schemes on structured (either Cartesian or smooth curvilinear) meshes have been quite mature, the development of WENO schemes on unstructured meshes has been less advanced, see Section 3.5. In particular, simple, efficient and robust WENO schemes for unstructured meshes in three dimensions still need a lot of investigation, see the preliminary results in [42, 43, 184].
4. The hybridizing of the WENO methodology with other types of schemes such as the WENO-compact schemes discussed in Section 5.2, the hybrid WENO-spectral scheme discussed in Section 5.3, and the WENO scheme within a multi-resolution framework discussed in Section 5.4, has the potential of producing schemes maintaining the advantages of both the WENO schemes and other types of schemes, and is worth further investigation. The application of the WENO methodology to other schemes, such as using WENO as a limiter for the discontinuous Galerkin method discussed in Section 5.1, is also a promising research direction.
5. The design of WENO schemes with special properties for specific applications, such as the well-balanced WENO schemes discussed in Section 3.5, will significantly enhance the applicability of WENO schemes to these specific applications. Along a similar line one could imagine designing WENO schemes which are uniformly accurate and stable for stiff perturbations from equilibriums.
6. The design of WENO schemes based on other than the polynomial building blocks would be beneficial. Polynomials are the simplest and in most situations adequate functions to use as building blocks for interpolation and reconstruction, however other types of functions, such as the radial basis functions, local exponential and local trigonometric functions may perform better in some applications. ENO schemes based on other than the polynomial building blocks were designed in [26]. Discontinuous Galerkin methods based on other than the polynomial approximation spaces were designed in [173]. Preliminary results on using polyharmonic splines in the WENO reconstruction

on unstructured meshes were given in [1]. Further research in this direction would be desirable.

7. Theoretical analysis of WENO schemes. While modifications to the schemes solely for the purpose of stability or convergence analysis without improvement to the actual computation should be discouraged (it should be especially discouraged if the modification destroys the self-similarity property of the scheme, see Section 3.5), any analysis to the unmodulated WENO schemes, even partial results, would be valuable. The convergence result for the Hamilton-Jacobi equations [13], reviewed in Section 4, is a good example of such analysis. It would be very interesting to see if similar results can be proved for a reasonable WENO scheme for specific conservation laws, see for example [122] for a weaker result requiring more restrictive reconstructions.
8. Application of the WENO idea to a wider class of problems. Since the essential idea of WENO is just an interpolation or reconstruction procedure which is not directly related to PDEs, we can imagine the application of this idea to non-PDE areas, such as image and signal processing, computer graphics, data and information processing, etc.

References

- [1] T. Aboiyar, E.H. Georgoulis and A. Iske, *High order WENO finite volume schemes using polyharmonic spline reconstruction*, Proceedings of the International Conference on Numerical Analysis and Approximation Theory (NAAT 2006), Cluj-Napoca, Romania, July 5-8, 2006, 113-126.
- [2] K. Alhumaizi, *Comparison of finite difference methods for the numerical simulation of reacting flow*, Computers and Chemical Engineering, 28 (2004), 1759-1769.
- [3] C. Appert, C. Tenaud, X. Chavanne, S. Balibar, F. Caupin and D. d'Humieres, *Nonlinear effects and shock formation in the focusing of a spherical acoustic wave - Numerical*

simulations and experiments in liquid helium, European Physical Journal B, 35 (2003), 531-549.

- [4] D. Balsara and C.-W. Shu, *Monotonicity preserving weighted essentially non-oscillatory schemes with increasingly high order of accuracy*, Journal of Computational Physics, 160 (2000), 405-452.
- [5] E. Bassano, *Level-set based numerical simulation of a migrating and dissolving liquid drop in a cylindrical cavity*, International Journal for Numerical Methods in Fluids, 44 (2004), 409-429.
- [6] E. Bassano and D. Castagnolo, *Marangoni migration of a methanol drop in cyclohexane matrix in a closed cavity*, Microgravity Science and Technology, 14 (2003), 20-33.
- [7] B.L. Bihari and A. Harten, *Application of generalized wavelets: a multiresolution scheme*, Journal of Computational Physics, 61 (1995), 275-321.
- [8] S. Bryson and D. Levy, *High-order central WENO schemes for multi-dimensional Hamilton-Jacobi equations*, SIAM Journal on Numerical Analysis, 41 (2003), 1339–1369.
- [9] R. Bürger and A. Kozakevicius, *Adaptive multiresolution WENO schemes for multi-species kinematic flow models*, Journal of Computational Physics, to appear.
- [10] M.J. Caceres, J.A. Carrillo and P. Degond, *The Child-Langmuir limit for semiconductors: A numerical validation*, Mathematical Modelling and Numerical Analysis, 36 (2002), 1161-1176.
- [11] M.J. Caceres, J.A. Carrillo, I. Gamba, A. Majorana and C-W. Shu, *DSMC versus WENO-BTE: a double gate MOSFET example*, Journal of Computational Electronics, to appear.

- [12] C. Canuto, M.Y. Hussaini, A. Quarteroni and T.A. Zang, *Spectral Methods in Fluid Dynamics*, Springer-Verlag, 1988.
- [13] E. Carlini, R. Ferretti and G. Russo, *A weighted essentially nonoscillatory, large time-step scheme for Hamilton-Jacobi equations*, SIAM Journal on Scientific Computing, 27 (2005), 1071-1091.
- [14] J.A. Carrillo, I.M. Gamba, A. Majorana and C.-W. Shu, *A WENO-solver for the transients of Boltzmann-Poisson system for semiconductor devices. Performance and comparisons with Monte Carlo methods*, Journal of Computational Physics, 184 (2003), 498-525.
- [15] J.A. Carrillo, I. Gamba, A. Majorana and C.-W. Shu, *2D semiconductor device simulations by WENO-Boltzmann schemes: efficiency, boundary conditions and comparison to Monte Carlo methods*, Journal of Computational Physics, 214 (2006), 55-80.
- [16] J.A. Carrillo and T. Goudon, *A numerical study on large-time asymptotics of the Lifshitz-Slyozov system*, Journal of Scientific Computing, 20 (2004), 69-113.
- [17] M. Castro, J.M. Gallardo and C. Parés, *High order finite volume schemes based on reconstruction of states for solving hyperbolic systems with nonconservative products. Application to shallow-water systems*, Mathematics of Computation, 75 (2006), 1103-1134.
- [18] J. Casper, C.-W. Shu and H.L. Atkins, *Comparison of two formulations for high-order accurate essentially nonoscillatory schemes*, AIAA Journal, 32 (1994), 1970-1977.
- [19] C. Cercignani, I. Gamba, J. Jerome and C.-W. Shu, *Device benchmark comparisons via kinetic, hydrodynamic, and high-field models*, Computer Methods in Applied Mechanics and Engineering, 181 (2000), 381-392.

- [20] D.P. Chen, R.S. Eisenberg, J.W. Jerome and C.-W. Shu, *Hydrodynamic model of temperature change in open ionic channels*, Biophysical Journal, 69 (1995), 2304-2322.
- [21] H. Chen and S.M. Liang, *Planar blast/vortex interaction and sound generation*, AIAA Journal 40 (2002), 2298-2304.
- [22] T.S. Cheng and K.S. Lee, *Numerical simulations of underexpanded supersonic jet and free shear layer using WENO schemes*, International Journal of Heat and Fluid Flow, 26 (2005), 755-770.
- [23] G. Chiavassa and R. Donat, *Point value multiscale algorithms for 2D compressive flows*, SIAM Journal on Scientific Computing, 23 (2001), 805-823.
- [24] C.-S. Chou and C.-W. Shu, *High order residual distribution conservative finite difference WENO schemes for steady state problems on non-smooth meshes*, Journal of Computational Physics, 214 (2006), 698-724.
- [25] C.-S. Chou and C.-W. Shu, *High order residual distribution conservative finite difference WENO schemes for convection-diffusion steady state problems on non-smooth meshes*, Journal of Computational Physics, to appear.
- [26] S. Christofi, *The study of building blocks for essentially non-oscillatory (ENO) schemes*, Ph.D. thesis, Division of Applied Mathematics, Brown University, 1996.
- [27] B. Cockburn, S. Hou and C.-W. Shu, *The Runge-Kutta local projection discontinuous Galerkin finite element method for conservation laws IV: the multidimensional case*, Mathematics of Computation, 54 (1990), 545-581.
- [28] B. Cockburn and C.-W. Shu, *TVB Runge-Kutta local projection discontinuous Galerkin finite element method for conservation laws II: general framework*, Mathematics of Computation, 52 (1989), 411-435.

- [29] B. Cockburn and C.-W. Shu, *Nonlinearly stable compact schemes for shock calculations*, SIAM Journal on Numerical Analysis, 31 (1994), 607-627.
- [30] B. Cockburn and C.-W. Shu, *The Runge-Kutta discontinuous Galerkin method for conservation laws V: multidimensional systems*, Journal of Computational Physics, 141 (1998), 199-224.
- [31] B. Cockburn and C.-W. Shu, *Runge-Kutta Discontinuous Galerkin methods for convection-dominated problems*, Journal of Scientific Computing, 16 (2001), 173-261.
- [32] B. Cockburn and C.-W. Shu, *Foreword for the special issue on discontinuous Galerkin method*, Journal of Scientific Computing, 22-23 (2005), 1-3.
- [33] P. Colella and P.R. Woodward, *The piecewise parabolic method (PPM) for gas dynamical simulations*, Journal of Computational Physics, 54 (1984), 174-201.
- [34] B. Costa and W.S. Don, *Multi-domain hybrid spectral-WENO methods for hyperbolic conservation laws*, Journal of Computational Physics, to appear.
- [35] B. Costa, W.S. Don, D. Gottlieb and R. Sendersky, *Two-dimensional multi-domain hybrid spectral-WENO methods for conservation laws*, Communications in Computational Physics, 1 (2006), 548-574.
- [36] N. Crnjaric-Zic, S. Vukovic and L. Sopta, *Extension of ENO and WENO schemes to one-dimensional sediment transport equations*, Computers and Fluids, 33 (2004), 31-56.
- [37] C. Dawson, *Foreword for the special issue on discontinuous Galerkin method*, Computer Methods in Applied Mechanics and Engineering, 195 (2006), 3183.
- [38] L. Del Zanna, M. Velli and P. Londrillo, *Dynamical response of a stellar atmosphere to pressure perturbations: numerical simulations*, Astronomy and Astrophysics, 330 (1998), L13-L16.

- [39] X. Deng and H. Zhang, *Developing high-order weighted compact nonlinear schemes*, Journal of Computational Physics, 165 (2000), 22-44.
- [40] B. Després and F. Lagoutière, *Contact discontinuity capturing schemes for linear advection and compressible gas dynamics*, Journal of Scientific Computing, 16 (2001), 479-524.
- [41] W.S. Don and D. Gottlieb, *Spectral simulation of supersonic reactive flows*, SIAM Journal on Numerical Analysis, 35 (1998), 2370-2384.
- [42] M. Dumbser and M. Käser, *Arbitrary high order non-oscillatory finite volume schemes on unstructured meshes for linear hyperbolic systems*, Journal of Computational Physics, to appear.
- [43] M. Dumbser, M. Käser, V.A. Titarev and E.F. Toro, *Quadrature-free non-oscillatory finite volume schemes on unstructured meshes for nonlinear hyperbolic systems*, Journal of Computational Physics, submitted.
- [44] L.-L. Feng, J. Pando and L.-Z. Fang, *Intermittent features of the quasar Ly alpha transmitted flux: Results from cosmological hydrodynamic simulations*, Astrophysical Journal, 587 (2003), 487-499.
- [45] L.-L. Feng, C.-W. Shu and M. Zhang, *A hybrid cosmological hydrodynamic/N-body code based on a weighted essentially non-oscillatory scheme*, Astrophysical Journal, 612 (2004), 1-13.
- [46] F. Filbet and C.-W. Shu, *Approximation of hyperbolic models for chemosensitive movement*, SIAM Journal on Scientific Computing, 27 (2005), 850-872.
- [47] J.L. Fisker and D.S. Balsara, *Simulating the boundary layer between a white dwarf and its accretion disk*, Astrophysical Journal, 635 (2005), L69-L72.

- [48] O. Friedrichs, *Weighted essentially non-oscillatory schemes for the interpolation of mean values on unstructured grids*, Journal of Computational Physics, 144 (1998), 194-212.
- [49] M. Galler and F. Schurrer, *A direct multigroup-WENO solver for the 2D non-stationary Boltzmann-Poisson system for GaAs devices: GaAs-MESFET*, Journal of Computational Physics, 212 (2006), 778-797.
- [50] S.K. Godunov, *A difference scheme for numerical computation of discontinuous solutions of equations of fluid dynamics*, Rossiiskaya Akademiya Nauk. Matematicheskii Sbornik (Mat. Sb.), 47 (1959), 271-306.
- [51] D. Gottlieb and S. Orszag, *Numerical Analysis of Spectral Methods: Theory and Applications*, SIAM-CBMS, Philadelphia, 1977.
- [52] D. Gottlieb and C.-W. Shu, *On the Gibbs phenomenon and its resolution*, SIAM Review, 39 (1997), 644-668.
- [53] S. Gottlieb, *Convergence to steady-state of weighted ENO schemes, norm preserving Runge-Kutta methods and a modified conjugate gradient method*, Ph.D. thesis, Division of Applied Mathematics, Brown University, 1998.
- [54] S. Gottlieb, D. Gottlieb and C.-W. Shu, *Recovering high order accuracy in WENO computations of steady state hyperbolic systems*, Journal of Scientific Computing, 28 (2006), 307-318.
- [55] S. Gottlieb, J.S. Mullen and S.J. Ruuth, *A fifth order flux implicit WENO method*, Journal of Scientific Computing, 27 (2006), 271-287.
- [56] S. Gottlieb, C.-W. Shu and E. Tadmor, *Strong stability preserving high order time discretization methods*, SIAM Review, 43 (2001), 89-112.

- [57] F. Grasso and S. Pirozzoli, *Shock-wave-vortex interactions: Shock and vortex deformations, and sound production*, Theoretical and Computational Fluid Dynamics, 13 (2000), 421-456.
- [58] F. Grasso and S. Pirozzoli, *Shock wave-thermal inhomogeneity interactions: Analysis and numerical simulations of sound generation*, Physics of Fluids, 12 (2000), 205-219.
- [59] Y. Ha, C.L. Gardner, A. Gelb and C.-W. Shu, *Numerical simulation of high Mach number astrophysical jets with radiative cooling*, Journal of Scientific Computing, 24 (2005), 597-612.
- [60] A. Hadjadj and A. Kudryavtsev, *Computation and flow visualization in high-speed aerodynamics*, Journal of Turbulence, 6(16) (2005), 1-25.
- [61] A. Harten, *High resolution schemes for hyperbolic conservation laws*, Journal of Computational Physics, 49 (1983), 357-393.
- [62] A. Harten: *ENO schemes with subcell resolution*, Journal of Computational Physics, 83 (1989), 148-184.
- [63] A. Harten, *Multiresolution algorithms for the numerical solution of hyperbolic conservation laws*, Communications on Pure and Applied Mathematics, 48 (1995), 1305-1342.
- [64] A. Harten, B. Engquist, S. Osher and S. Chakravarthy, *Uniformly high order essentially non-oscillatory schemes, III*, Journal of Computational Physics, 71 (1987), 231-303.
- [65] A. Harten, S. Osher, B. Engquist and S. Chakravarthy, *Some results on uniformly high order accurate essentially non-oscillatory schemes*, Applied Numerical Mathematics, 2 (1986), 347-377.
- [66] P. He, J. Liu, L.-L. Feng, C.-W. Shu and L.-Z. Fang, *Low-redshift cosmic baryon fluid on large scales and She-Leveque universal scaling*, Physical Review Letters, 96 (2006), 051302.

- [67] X. He and A.R. Karagozian, *Numerical simulation of pulse detonation engine phenomena*, Journal of Scientific Computing, 19 (2003), 201-224.
- [68] A.K. Henrick, T.D. Aslam and J.M. Powers, *Mapped weighted essentially non-oscillatory schemes: Achieving optimal order near critical points*, Journal of Computational Physics, 207 (2005), 542-567.
- [69] A.K. Henrick, T.D. Aslam and J.M. Powers, *Simulations of pulsating one-dimensional detonations with true fifth order accuracy*, Journal of Computational Physics, 213 (2006), 311-329.
- [70] R. Hirsh, *Higher order accurate difference solutions of fluid mechanics problems by a compact differencing technique*, Journal of Computational Physics, 19 (1975), 90-109.
- [71] C. Hu and C.-W. Shu, *Weighted essentially non-oscillatory schemes on triangular meshes*, Journal of Computational Physics, 150 (1999), 97-127.
- [72] X.Y. Hu, D.L. Zhang, B.C. Khoo and Z.L. Jiang, *The structure and evolution of a two-dimensional H-2/O-2/Ar cellular detonation*, Shock Waves, 14 (2005), 37-44.
- [73] L. Huang, S.C. Wong, M. Zhang, C.-W. Shu and W.H.K. Lam, *A reactive dynamic user equilibrium model for pedestrian flows: a continuum modeling approach*, submitted to Transportation Research Part B.
- [74] P. Jamkhedkar, L.-L. Feng, W. Zheng and L.-Z. Fang, *Power spectrum and intermittency of Ly alpha transmitted flux of QSO HE 2347-4342*, Astrophysical Journal, 633 (2005), 52-60.
- [75] G. Jiang and D.-P. Peng, *Weighted ENO schemes for Hamilton-Jacobi equations*, SIAM Journal on Scientific Computing, 21 (2000), 2126-2143.
- [76] G. Jiang and C.-W. Shu, *Efficient implementation of weighted ENO schemes*, Journal of Computational Physics, 126 (1996), 202-228.

- [77] G. Jiang and C.-C. Wu, *A high order WENO finite difference scheme for the equations of ideal magnetohydrodynamics*, Journal of Computational Physics, 150 (1999), 561-594.
- [78] L. Jiang, M. Choudhari, C.L. Chang and C.Q. Liu, *Direct numerical simulations of instability-wave generation and propagation in supersonic boundary layers*, Lecture Notes in Computer Science, 2668 (2003), 859-870.
- [79] L. Jiang, H. Shan and C.Q. Liu, *Weighted compact scheme for shock capturing*, International Journal of Computational Fluid Dynamics, 15 (2001), 147-155.
- [80] K. Kremeyer, K. Sebastian and C.-W. Shu, *Computational study of shock mitigation and drag reduction by pulsed energy lines*, AIAA Journal, 44 (2006), 1720-1731.
- [81] S. Labrunie, J.A. Carrillo and P. Bertrand, *Numerical study on hydrodynamic and quasi-neutral approximations for collisionless two-species plasmas* Journal of Computational Physics, 200 (2004), 267-298.
- [82] F. Ladeinde, X.D. Cai, M.R. Visbal and D.V. Gaitonde, *Turbulence spectra characteristics of high order schemes for direct and large eddy simulation*, Applied Numerical Mathematics, 36 (2001), 447-474.
- [83] P. Lax and M. Mock, *The computation of discontinuous solutions of linear hyperbolic equations*, Communications on Pure and Applied Mathematics, 31 (1978), 423-430.
- [84] T.K. Lee, X.L. Zhong, L. Gong and R. Quinn, *Hypersonic aerodynamic heating prediction using weighted essentially nonoscillatory schemes*, Journal of Spacecraft and Rockets, 40 (2003), 294-298.
- [85] S. Lele, *Compact finite difference schemes with spectral-like resolution*, Journal of Computational Physics, 103 (1992), 16-42.

- [86] R.J. LeVeque, *Numerical Methods for Conservation Laws*, Birkhauser Verlag, Basel, 1990.
- [87] D. Levy, S. Nayak, C.-W. Shu and Y.-T. Zhang, *Central WENO schemes for Hamilton-Jacobi equations on triangular meshes*, SIAM Journal on Scientific Computing, to appear.
- [88] D. Levy, G. Puppo and G. Russo, *Central WENO schemes for hyperbolic systems of conservation laws*, Mathematical Modelling and Numerical Analysis (M^2AN), 33 (1999), 547-571.
- [89] D. Levy, G. Puppo and G. Russo, *Compact central WENO schemes for multidimensional conservation laws*, SIAM Journal on Scientific Computing, 22 (2000), 656-672.
- [90] D. Levy, G. Puppo and G. Russo, *A third order central WENO scheme for 2D conservation laws*, Applied Numerical Mathematics, 33 (2000), 415-421.
- [91] Y. Li and F. Raichlen, *Non-breaking and breaking solitary wave run-up*, Journal of Fluid Mechanics, 456 (2002), 295-318.
- [92] S. Liang and H. Chen, *Numerical simulation of underwater blast-wave focusing using a high-order scheme*, AIAA Journal, 37 (1999), 1010-1013.
- [93] S.M. Liang, W.T. Chung, H. Chen and S.H. Shyu, *Numerical investigation of reflected shock/vortex interaction near an open-ended duct* AIAA Journal, 43 (2005), 349-356.
- [94] S.M. Liang and C.P. Lo, *Shock/vortex interactions induced by blast waves*, AIAA Journal, 41 (2003), 1341-1346.
- [95] Y.I. Lim, J.M. Le Lann and X. Joulia, *Accuracy, temporal performance and stability comparisons of discretization methods for the numerical solution of partial differential equations (PDEs) in the presence of steep moving fronts*, Computers and Chemical Engineering, 25 (2001), 1483-1492.

- [96] Y.I. Lim, J.M. Le Lann, X.M. Meyer, X. Joulia, G. Lee, E.S. Yoon, *On the solution of population balance equations (PBE) with accurate front tracking methods in practical crystallization processes*, Chemical Engineering Science, 57 (2002), 3715-3732.
- [97] G. Lin, C.H. Su and G.E. Karniadakis, *The stochastic piston problem*, Proceedings of the National Academy of Sciences of the United States of America, 101 (2004), 15840-15845.
- [98] S.Y. Lin and J.J. Hu, *Parametric study of weighted essentially nonoscillatory schemes for computational aeroacoustics*, AIAA Journal, 39 (2001), 371-379.
- [99] R. Liska and B. Wendroff, *Composite schemes for conservation laws*, SIAM Journal on Numerical Analysis, 35 (1998), 2250-2271.
- [100] R. Liska and B. Wendroff, *Two-dimensional shallow water equations by composite schemes*, International Journal for Numerical Methods in Fluids, 30 (1999), 461-479.
- [101] X.-D. Liu, S. Osher and T. Chan, *Weighted essentially non-oscillatory schemes*, Journal of Computational Physics, 115 (1994), 200-212.
- [102] B. Lombard and R. Donat, *The explicit simplified interface method for compressible multicomponent flows* SIAM Journal on Scientific Computing, 27 (2005), 208-230.
- [103] A. Majda and S. Osher, *Propagation of error into regions of smoothness for accurate difference approximations to hyperbolic equations*, Communications on Pure and Applied Mathematics, 30 (1977), 671-705.
- [104] A. Marquina and P. Mulet, *A flux-split algorithm applied to conservative models for multicomponent compressible flows*, Journal of Computational Physics, 185 (2003), 120-138.

- [105] M.P. Martin, E.M. Taylor, M. Wu and V.G. Weirs, *A bandwidth-optimized WENO scheme for the direct numerical simulation of compressible turbulence*, Journal of Computational Physics, to appear.
- [106] B. Merryman, *Understanding the Shu-Osher conservative finite difference form*, Journal of Scientific Computing, 19 (2003), 309-322.
- [107] P. Montarnal and C.-W. Shu, *Real gas computation using an energy relaxation method and high order WENO schemes*, Journal of Computational Physics, 148 (1999), 59-80.
- [108] A.S. Mouronval and A. Hadjadj, *Numerical study of the starting process in a supersonic nozzle*, Journal of Propulsion and Power, 21 (2005), 374-378.
- [109] H. Nessyahu and E. Tadmor, *Non-oscillatory central differencing for hyperbolic conservation laws*, Journal of Computational Physics, 87 (1990), 408-463.
- [110] S. Noelle, N. Pankratz, G. Puppo and J.R. Natvig, *Well-balanced finite volume schemes of arbitrary order of accuracy for shallow water flows*, Journal of Computational Physics, 213 (2006), 474-499.
- [111] S. Noelle, Y. Xing and C.-W. Shu, *High order well-balanced finite volume WENO schemes for shallow water equation with moving water*, submitted to Journal of Computational Physics.
- [112] R.R. Nourgaliev, T.N. Dinh and T.G. Theofanous, *A pseudocompressibility method for the numerical simulation of incompressible multifluid flows*, International Journal of Multiphase Flow, 30 (2004), 901-937.
- [113] S. Osher and R. Fedkiw, *Level Set Methods and Dynamic Implicit Surfaces*, Springer-Verlag, New York, 2003.
- [114] S. Osher and C.-W. Shu, *High-order essentially nonoscillatory schemes for Hamilton-Jacobi equations*, SIAM Journal on Numerical Analysis, 28 (1991), 907-922.

- [115] S. Pirozzoli, *Conservative hybrid compact-WENO schemes for shock-turbulence interaction*, Journal of Computational Physics, 178 (2002), 81-117.
- [116] S. Pirozzoli, *Dynamics of ring vortices impinging on planar shock waves*, Physics of Fluids, 16 (2004), 1171-1185.
- [117] S. Pirozzoli, F. Grasso and A. D'Andrea, *Interaction of a shock wave with two counter-rotating vortices: Shock dynamics and sound production*, Physics of Fluids, 13 (2001), 3460-3481.
- [118] S. Pirozzoli, F. Grasso and T.B. Gatski, *Direct numerical simulation and analysis of a spatially evolving supersonic turbulent boundary layer at $M=2.25$* , Physics of Fluids, 16 (2004), 530-545.
- [119] D. Ponziani, S. Pirozzoli and F. Grasso, *Development of optimized weighted-ENO schemes for multiscale compressible flows*, International Journal for Numerical Methods in Fluids, 42 (2003), 953-977.
- [120] G. Puppo and G. Russo, *Staggered finite difference schemes for conservation laws*, Journal of Scientific Computing, 27 (2006), 403-418.
- [121] J.-M. Qiu, L.-L. Feng, C.-W. Shu and L.-Z. Fang, *A WENO algorithm of the temperature and ionization profiles around a point source*, New Astronomy, to appear.
- [122] J.-M. Qiu and C.-W. Shu, *Convergence of Godunov-type schemes for scalar conservation laws under large time steps*, submitted to SIAM Journal on Numerical Analysis.
- [123] J.-M. Qiu, C.-W. Shu, L.-L. Feng and L.-Z. Fang, *A WENO algorithm for the radiative transfer and ionized sphere at reionization*, New Astronomy, 12 (2006), 1-10.
- [124] J.-X. Qiu and C.-W. Shu, *On the construction, comparison, and local characteristic decomposition for high order central WENO schemes*, Journal of Computational Physics, 183 (2002), 187-209.

- [125] J.-X. Qiu and C.-W. Shu, *Finite difference WENO schemes with Lax-Wendroff type time discretization*, SIAM Journal on Scientific Computing, 24 (2003), 2185-2198.
- [126] J.-X. Qiu and C.-W. Shu, *Hermite WENO schemes and their application as limiters for Runge-Kutta discontinuous Galerkin method: one dimensional case*, Journal of Computational Physics, v193 (2003), 115-135.
- [127] J.-X. Qiu and C.-W. Shu, *Runge-Kutta discontinuous Galerkin method using WENO limiters*, SIAM Journal on Scientific Computing, v26 (2005), pp.907-929.
- [128] J.-X. Qiu and C.-W. Shu, *A comparison of troubled-cell indicators for Runge-Kutta discontinuous Galerkin methods using weighted essentially nonoscillatory limiters*, SIAM Journal on Scientific Computing, v27 (2005), pp.995-1013.
- [129] J.-X. Qiu and C.-W. Shu, *Hermite WENO schemes and their application as limiters for Runge-Kutta discontinuous Galerkin method II: two dimensional case*, Computers and Fluids, 34 (2005), 642-663.
- [130] J.-X. Qiu and C.-W. Shu, *Hermite WENO schemes for Hamilton-Jacobi equations*, Journal of Computational Physics, 204 (2005), 82-99.
- [131] A. Rault, G. Chiavassa and R. Donat, *Shock-vortex interactions at high Mach numbers*, Journal of Scientific Computing, 19 (2003), 347-371.
- [132] P. Roe, *Approximate Riemann solvers, parameter vectors and difference schemes*, Journal of Computational Physics, 27 (1978), 1-31.
- [133] T. Schuller, S. Ducruix, D. Durox, S. Candel, *Modeling tools for the prediction of premixed flame transfer functions*, Proceedings of the Combustion Institute, 29 (2003), 107-113.

- [134] T. Schuller, D. Durox and S. Candel, *A unified model for the prediction of laminar flame transfer functions: comparisons between conical and V-flame dynamics*, Combustion and Flame, 134 (2003), 21-34.
- [135] K. Sebastian and C.-W. Shu, *Multi domain WENO finite difference method with interpolation at sub-domain interfaces*, Journal of Scientific Computing, 19 (2003), 405-438.
- [136] S. Serna and A. Marquina, *Power ENO methods: a fifth-order accurate weighted power ENO method*, Journal of Computational Physics, 194 (2004), 632-658.
- [137] J. Shen, C.-W. Shu and M. Zhang, *High resolution schemes for a hierarchical size-structured model*, SIAM Journal on Numerical Analysis, to appear.
- [138] J. Shen, C.-W. Shu and M. Zhang, *High order WENO schemes for a hierarchical size-structured model*, in preparation.
- [139] J. Shi, C. Hu and C.-W. Shu, *A technique of treating negative weights in WENO schemes*, Journal of Computational Physics, 175 (2002), 108-127.
- [140] J. Shi, Y.-T. Zhang and C.-W. Shu, *Resolution of high order WENO schemes for complicated flow structures*, Journal of Computational Physics, 186 (2003), 690-696.
- [141] C.-W. Shu, *Total-Variation-Diminishing time discretizations*, SIAM Journal on Scientific and Statistical Computing, 9 (1988), 1073-1084.
- [142] C.-W. Shu, *Essentially non-oscillatory and weighted essentially non-oscillatory schemes for hyperbolic conservation laws*, in *Advanced Numerical Approximation of Nonlinear Hyperbolic Equations*, B. Cockburn, C. Johnson, C.-W. Shu and E. Tadmor (Editor: A. Quarteroni), Lecture Notes in Mathematics, volume 1697, Springer, 1998, 325-432.
- [143] C.-W. Shu, *High order ENO and WENO schemes for computational fluid dynamics*, in *High-Order Methods for Computational Physics*, T.J. Barth and H. Deconinck, editors,

Lecture Notes in Computational Science and Engineering, volume 9, Springer, 1999, 439-582.

- [144] C.-W. Shu, *High order finite difference and finite volume WENO schemes and discontinuous Galerkin methods for CFD*, International Journal of Computational Fluid Dynamics, 17 (2003), 107-118.
- [145] C.-W. Shu, W.-S. Don, D. Gottlieb, O. Schilling and L. Jameson, *Numerical convergence study of nearly-incompressible, inviscid Taylor-Green vortex flow*, Journal of Scientific Computing, 24 (2005), 569-595.
- [146] C.-W. Shu and S. Osher, *Efficient implementation of essentially non-oscillatory shock capturing schemes*, Journal of Computational Physics, 77 (1988), 439-471.
- [147] C.-W. Shu and S. Osher, *Efficient implementation of essentially non-oscillatory shock capturing schemes, II*, Journal of Computational Physics, 83 (1989), 32-78.
- [148] C.-W. Shu, T.A. Zang, G. Erlebacher, D. Whitaker and S. Osher, *High-order ENO schemes applied to two- and three-dimensional compressible flow*, Applied Numerical Mathematics, 9 (1992), 45-71.
- [149] B.A. Steve and D. Levy, *High-order semi-discrete central-upwind schemes for multi-dimensional Hamilton-Jacobi equations*, Journal of Computational Physics, 189 (2003), 63-87.
- [150] G. Strang, *Accurate partial difference schemes II. Nonlinear problems*, Numerische Mathematik, 6 (1964), 37-46.
- [151] D.C. Sun, C.B. Hu and T.M. Cai, *Computation of supersonic turbulent flowfield with transverse injection*, Applied Mathematics and Mechanics-English Edition, 23 (2002), 107-113.

- [152] M. Sussman, P. Smereka and S. Osher, *A level set approach for computing solutions to incompressible two-phase flow*, Journal of Computational Physics, 114 (1994), 146-159.
- [153] C.K.W. Tam and J.C. Webb, *Dispersion-relation-preserving finite difference schemes for computational acoustics*, Journal of Computational Physics, 107 (1993), 262-281.
- [154] S. Teramoto, *Large eddy simulation of shock wave boundary layer interaction*, Transactions of the Japan Society for Aeronautical and Space Sciences, 47 (2005), 268-275.
- [155] V.A. Titarev and E.F. Toro, *ADER: arbitrary high order Godunov approach*, Journal of Scientific Computing, 17 (2002), 609-618.
- [156] E.F. Toro, *Riemann solvers and numerical methods for fluid dynamics, a practical introduction*, Springer, Berlin, 1997.
- [157] B. van Leer, *Towards the ultimate conservative difference scheme V. A second order sequel to Godunov's method*, Journal of Computational Physics, 32 (1979), 101-136.
- [158] S. Vukovic and L. Sopta, *ENO and WENO schemes with the exact conservation property for one-dimensional shallow water equations*, Journal of Computational Physics, 179 (2002), 593-621.
- [159] Z.J. Wang and R.F. Chen, *Optimized weighted essentially nonoscillatory schemes for linear waves with discontinuity*, Journal of Computational Physics, 174 (2001), 381-404.
- [160] C.C. Wu and T. Chang, *Dynamical evolution of coherent structures in intermittent two-dimensional MHD turbulence*, IEEE Transactions on Plasma Science, 28 (2000), 1938-1943.
- [161] Y. Xing and C.-W. Shu, *High order finite difference WENO schemes with the exact conservation property for the shallow water equations*, Journal of Computational Physics, 208 (2005), 206-227.

- [162] Y. Xing and C.-W. Shu, *High order well-balanced finite difference WENO schemes for a class of hyperbolic systems with source terms*, Journal of Scientific Computing, 27 (2006), 477-494.
- [163] Y. Xing and C.-W. Shu, *High order well-balanced finite volume WENO schemes and discontinuous Galerkin methods for a class of hyperbolic systems with source terms*, Journal of Computational Physics, 214 (2006), 567-598.
- [164] Y. Xing and C.-W. Shu, *A new approach of high order well-balanced finite volume WENO schemes and discontinuous Galerkin methods for a class of hyperbolic systems with source terms*, Communications in Computational Physics, 1 (2006), 101-135.
- [165] Z. Xu and C.-W. Shu, *Anti-diffusive flux corrections for high order finite difference WENO schemes*, Journal of Computational Physics, 205 (2005), 458-485.
- [166] Z. Xu and C.-W. Shu, *Anti-diffusive high order WENO schemes for Hamilton-Jacobi equations*, Methods and Applications of Analysis, 12 (2005), 169-190.
- [167] Z. Xu and C.-W. Shu, *Anti-diffusive finite difference WENO methods for shallow water with transport of pollutant*, Journal of Computational Mathematics, 24 (2006), 239-251.
- [168] C. Yang and Z.S. Mao, *Numerical simulation of interphase mass transfer with the level set approach*, Chemical Engineering Science, 60 (2005), 2643-2660.
- [169] H. Yang, *An artificial compression method for ENO schemes: the slope modification method*, Journal of Computational Physics, 89 (1990), 125-160.
- [170] J.Y. Yang, Y.C. Perng and R.H. Yen, *Implicit weighted essentially nonoscillatory schemes for the compressible Navier-Stokes equations*, AIAA Journal, 39 (2001), 2082-2090.

- [171] J.Y. Yang, S. Yang, Y. Chen and C. Hsu, *Implicit weighted ENO schemes for the three-dimensional incompressible Navier-Stokes equations*, Journal of Computational Physics, 146 (1998), 464-487.
- [172] J.Y. Yang, R.H. Yen and Y.C. Perng, *Three-dimensional wing flow computations using implicit WENO Euler solvers*, Journal of Aircraft, 39 (2002), 181-184.
- [173] L. Yuan and C.-W. Shu, *Discontinuous Galerkin method based on non-polynomial approximation spaces*, Journal of Computational Physics, 218 (2006), 295-323.
- [174] N.J. Zabusky, S. Gupta and Y. Gulak, *Localization and spreading of contact discontinuity layers in simulations of compressible dissipationless flows*, Journal of Computational Physics, 188 (2003), 348-364.
- [175] M. Zhang, C.-W. Shu, G.C.K. Wong and S.C. Wong, *A weighted essentially non-oscillatory numerical scheme for a multi-class Lighthill-Whitham-Richards traffic flow model*, Journal of Computational Physics, 191 (2003), 639-659.
- [176] P. Zhang, S.C. Wong and C.-W. Shu, *A weighted essentially non-oscillatory numerical scheme for a multi-class traffic flow model on an inhomogeneous highway*, Journal of Computational Physics, 212 (2006), 739-756.
- [177] Q. Zhang, M. Zhang, G. Jin, D. Liu and C.-W. Shu, *Modeling, numerical methods and simulation for particle-fluid two phase flow problems*, Computers and Mathematics with Applications, 47 (2004), 1437-1462.
- [178] S. Zhang and C.-W. Shu, *A new smoothness indicator for the WENO schemes and its effect on the convergence to steady state solutions*, Journal of Scientific Computing, to appear.
- [179] S. Zhang, Y.-T. Zhang and C.-W. Shu, *Multi-stage interaction of a shock wave and a strong vortex*, Physics of Fluids, 17 (2005), 116101.

- [180] S. Zhang, Y.-T. Zhang and C.-W. Shu, *Interaction of a shock wave with an oblique vortex pair: shock dynamics and mechanism of sound generation*, Physics of Fluids, 18 (2006), 126101.
- [181] W. Zhang and A. MacFadyen, *RAM: A relativistic adaptive mesh refinement hydrodynamics code*, Astrophysical Journal Supplement Series, 164 (2006), 255-279.
- [182] Y.-T. Zhang, J. Shi, C.-W. Shu and Y. Zhou, *Numerical viscosity and resolution of high-order weighted essentially nonoscillatory schemes for compressible flows with high Reynolds numbers*, Physical Review E, 68 (2003), 046709.
- [183] Y.-T. Zhang and C.-W. Shu, *High order WENO schemes for Hamilton-Jacobi equations on triangular meshes*, SIAM Journal on Scientific Computing, 24 (2003), 1005-1030.
- [184] Y.-T. Zhang and C.-W. Shu, *High order WENO schemes for three dimensional tetrahedral meshes*, in preparation.
- [185] Y.-T. Zhang, C.-W. Shu and Y. Zhou, *Effects of shock waves on Rayleigh-Taylor instability*, Physics of Plasmas, 13 (2006), 062705.
- [186] Y.-T. Zhang, H.-K. Zhao and J. Qian, *High order fast sweeping methods for static Hamilton-Jacobi equations*, Journal of Scientific Computing, 29 (2006), 25-56.
- [187] T. Zhou, Y. Li and C.-W. Shu, *Numerical comparison of WENO finite volume and Runge-Kutta discontinuous Galerkin methods*, Journal of Scientific Computing, 16 (2001), 145-171.